The size-mobility relationship of ions, aerosols, and other charged particle matter.

Carlos Larriba-Andaluz[1,*] and Francesco Carbone[2]

[1] Department of Energy and Mechanical Engineering, IUPUI, Indianapolis, IN, 46206
[2] Department of Mechanical Engineering, University of Connecticut, Storrs, CT, 06269

*corresponding autor. Email: clarriba@iupui.edu

Abstract

Electrical Mobility is arguably the property upon which some of the most successful classification criteria are based for aerosol particles and ions in the gas phase. Once the value of mobility is empirically obtained, it can be related to a geometrical descriptor of the charged entity through a size-mobility relationship. Given the multiscale range of sizes in the aerosol field, approaches that can provide accurate transformations from mobility to size are not straightforward, and many times rely on experimentally derived parameters. The most well-known size-mobility analytical expression covering the whole Knudsen range for spherical particles is the semi-empirical Stokes-Millikan correlation. This expression matches Stokes' drag friction coefficient in the continuum regime and the friction factor for a predominantly diffuse reemission of the gas molecule in the free molecular regime, as theorized by Epstein, with empirical slip coefficients chosen to agree with Millikan's oil drop experiments. Despite its success, the Stokes-Millikan correlation has its shortcomings. For example, it needs to be modified to predict the mobility of non-spherical entities and needs correction terms when potential interactions or reduced mass effects are non-negligible. The Stokes-Millikan asymptotic behavior also fails to predict the gradual transition from diffuse to specular reemission behavior that is observed for increasingly smaller ions within the free molecular regime. Here we make an attempt at providing a comprehensive account of the existing mass-mobility relations in the continuum, transition and free molecular regimes for both spherical and non-spherical particles. Epstein's diffuse interaction is critically explored experimentally and numerically for different gases in the free molecular regime with the observation that, as the size of the particle increases, a progression from specular to diffuse reemission occurs for all gases studied. The rate at which this variation happens seems to differ from gas to gas and to be related to the conditions for which diffuse reemission effects stem from a combination of scattering and potential interactions.

Keywords: Electrical Mobility; Transport Phenomena; Stokes-Millikan; Kinetic Theory; Ions; transition regime; free molecular regime

---

This is the author's manuscript of the article published in final edited form as:

Larriba-Andaluz, C., & Carbone, F. (2021). The size-mobility relationship of ions, aerosols, and other charged particle matter. Journal of Aerosol Science, 151, 105659. https://doi.org/10.1016/j.jaerosci.2020.105659

Nomenclature

Variable	Significance
$\boldsymbol{a}$	Radius of a sphere on an aggregate
$\boldsymbol{A_1, A_2, A_3/A, B, c}$	Slip Correction parameters
$\boldsymbol{b}$	Impact parameter
$\boldsymbol{B_{ij}}$	Drag force tensor
$\boldsymbol{\bar{c}}$	Gas average molecular speed
$\boldsymbol{c_i, c}$	Gas thermal velocity
$\boldsymbol{c_1, c_2}$	Phillips accommodation constants
$\boldsymbol{D}$	Diffusion coefficient
$\boldsymbol{d_H}$	Hydrodynamic diameter
$\boldsymbol{d_g}$	Diameter of the gas
$\boldsymbol{d_p}$	Particle mobility diameter
$\boldsymbol{d_{p,eff}}$	Effective diameter considering potential interaction enhancement
$\boldsymbol{d_{ve}}$	Volume equivalent diameter
$\boldsymbol{E}$	Electrical field
$\boldsymbol{F_D}$	Drag force
$\boldsymbol{f_f}$	Friction factor
$\boldsymbol{f(c_i)}$	Gas velocity distribution
$\boldsymbol{F(z_i)}$	Ion/Charged particle velocity distribution
$\boldsymbol{g_i, g}$	Relative velocity
$\boldsymbol{k}$	Boltzmann's Constant
$\boldsymbol{K_n}$	Knudsen number
$\boldsymbol{m_{gas}}$	Molecular mass of the gas
$\boldsymbol{m_{red}}$	Reduced Mass
$\boldsymbol{m_w}$	Molecular mass of the charged entity
$\boldsymbol{n}$	Gas number concentration
$\boldsymbol{N_A}$	Avogadro's number
$\boldsymbol{\overline{\overline{nn}}, \bar{\bar{I}}}$	Normal and unit dyadics
$\boldsymbol{n_\alpha}$	Concentration fraction leaving the particle surface accommodated
$\boldsymbol{n_i, t_{1,i}, t_{2,i}}$	Normal and tangential
$\boldsymbol{N_t}$	Total number of gas molecules entering a given domain in time τ_t
$\boldsymbol{p}$	Gas pressure
$\boldsymbol{PA}$	Orientationally averaged Projected Area
$\boldsymbol{\dot{p}_j^-, \dot{p}_j^+}$	Momentum of impinging and reflected molecules per unit time
$\boldsymbol{Q}$	Gas molecule flux
$\boldsymbol{q_i}$	Charge or partial charge in the particle
$\boldsymbol{q_1, q_2}$	Perturbations due to the presence of the sphere
$\boldsymbol{r}$	Distance between different entities
$\boldsymbol{R, R_0}$	Distance between force center and gas molecule, apsidal distance
$\boldsymbol{T_{\mathrm{eff}}}$	Effective temperature
$\boldsymbol{T_{l,k}}$	Oseen/Rotne and Pragers hydrodynamic tensor
$\boldsymbol{u_i}$	Perturbed velocity field over a sphere
$\boldsymbol{U_{pol}}$	Ion induced dipole potential interaction
$\boldsymbol{U_\infty}$	Free stream velocity
$\boldsymbol{v_d}$	Drift velocity
$\boldsymbol{V_m}$	Gas molar volume
$\boldsymbol{V_p}$	Gas molecule volume
$\boldsymbol{W_i}$	Center of mass velocity

ze	Particle charge; z elementary charges
z_i, z	Ion/Charged particle velocity
Z_p, K	Electrical Mobility
Z_{pfreem}	Electrical Mobility Free Molecular
$Z_{pcont}/Z_{continuum}$	Electrical Mobility in the continuum

Greek symbols

α	Accommodation coefficient
α_p	Polarization potential
$\alpha_T, \alpha_Q, \alpha_L$	Thermal diffusion factors
β_{ij}	Collision frequency
Δ	Correction to diffusion
$\zeta_1, \zeta_2, \zeta_3$	Annis slip correction coefficients
η	Viscosity
$\mathcal{L}$	Potential correction factor
λ	Mean free path of the gas
ξ	Accommodation enhancement factor
σ, ϵ	Lennard-Jones parameters, zero cross and well depth
Σ	Charged particle surface area
τ_t	Total time for N_t to enter the given domain
Φ	Gas-Charged particle Interaction Potential
φ_e	Ion induced dipole potential dimensionless interaction potential
ϕ, θ, γ	Orientation angle
χ_{def}	Deflection angle
χ_k	Collision frequency correction factor.
χ_m	Dynamic Shape factor
$\bar{\Omega}_{1,1}, \bar{\Omega}_{Teff}(1,1)$	Collision Cross Section/ First Collision Integral

1. Introduction

One of the most difficult challenges in the aerosol field is the classification of airborne particles due to their large disparity in mass, size, shape, composition, and concentration. Although it only pertains to the charged portion of particles suspended in air, one of the most successful classification criteria is that of separation by means of electrical mobility (Hoppel, Frick, & Larson, 1986; Knutson & Whitby, 1975; Wiedensohler, 1988). Fortunately, most ordinary aerosols can be charged in the gas phase in a predetermined and controlled manner, which has allowed the technique to become widespread. Electrical mobility, Z_p, as its name suggests, is a property that refers to the ability of a charged particle to be transported through a buffer gas by means of an electrical field. In its simplest one-dimensional definition, it is related to the electric field, E, through the drift velocity, v_d, as:

$$v_d = Z_p E \tag{1}$$

The electrical mobility is generally related to what is known as a mobility diameter which may then be compared to a physical size of the particle. This comparison, while useful to interpret data in a clean way, does convey an inevitable loss of information that might ultimately lead to wrong comparisons.

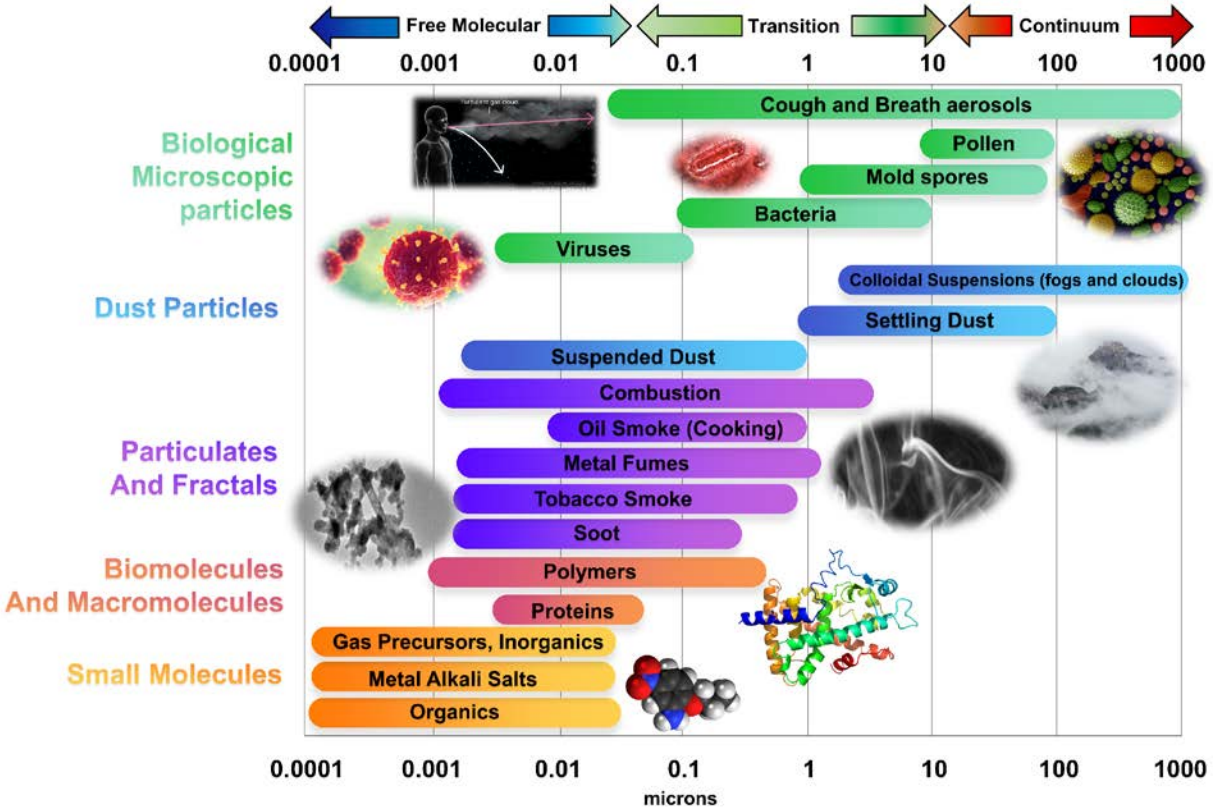

Figure 1. Multiscale range of particle sizes in the field of aerosols including the different regimes assuming standard pressure.

Among the complications surrounding particle classification within the realm of aerosols using electrical mobility, one of the most challenging aspects is the large multiscale range of different sizes and shapes, which extends from the free molecular to the continuum regime as shown in Figure 1. In particular, much of the particulate matter is just as likely to be much smaller or much larger than the gas mean free path, including all possible intermediate situations, which ultimately leads to a non-trivial characterization. While the particle in the free molecular regime is assumed to not perturb the gas and follow deterministic

formulations, the postulation completely changes as the particle becomes larger and a compression/rarefaction process ensues in the transition to continuum regimes. Because of such drastically different behaviors between the two different regimes, the difficulty resides in understanding how electrical mobility transitions smoothly from one extreme to the other, or, in other words, discerning how the mobility behaves as the particle size relates to the mean free path, λ. The ratio between the two is referred to as the Knudsen number ($Kn = 2\lambda/d_p$), where for Kn>>1 the particle does not perturb the gas and is considered to be in the free molecular regime whereas for Kn<<1, the particle is considered to be in the continuum. Therefore, an intricate relationship between electrical mobility and Knudsen number unequivocally must appear in the study of aerosols and its effect must be studied carefully.

A useful way to understand why molecular ions and macroscale charged particles behave in such different ways is to study how the drag force, or rather the friction factor f_f, behaves in the different regimes. The drag force, F_D, for a particle of mobility diameter d_p in the creeping flow continuum regime, without slip, is given by the well-known Stokes' law (Stokes, 1851):

$$F_D = 3\pi\eta d_p v_d = f_f v_d \tag{2}$$

where η is the viscosity of the gas. The appearance of a constant v_d in eq. (2) suggests that a steady state condition has been achieved between drag and electric force on a particle of charge ze ($F_e = zeE$), which allows a definition of the electrical mobility in the continuum given by:

$$Z_{p_{cont}} = \frac{ze}{3\pi\eta d_p} \tag{3}$$

In the free molecular regime, on the other hand, an approximation to the electrical mobility, more commonly referred to as ion mobility (and many times represented by K instead of Z_p), is given through kinetic theory:

$$Z_{p_{freem}} = \frac{3ze}{16n}\left(\frac{2\pi}{m_{red}kT_{eff}}\right)^{1/2}\frac{1}{\bar{\Omega}_{1,1}(T_{eff})} \tag{4}$$

which is known as the 2 temperature-theory Mason-Schamp (sometimes Mason-Viehland) equation (Edward A Mason & Schamp Jr, 1958; Larry A Viehland & Mason, 1978). Here n is the gas number concentration, k is the Boltzmann constant, T_{eff} is the effective temperature, $m_{red} = m_{gas}m_w/(m_{gas} + m_w)$ is the reduced mass of the gas/charged particle system with m_{gas} being the molecular mass of the gas and m_w the molecular mass of the charged particle, and $\bar{\Omega}_{1,1}(T_{eff})$ is the Collision Cross Section (CCS). The effective temperature includes collisional heating due to drift, $T_{eff} = T + m_{gas}v_d^2/3k$, where T is the equilibrium temperature of the buffer gas(Wannier, 1953). Under most scenarios pertaining to low velocity aerosols, the second term on the right-hand side, $m_{gas}v_d^2/3k$, is negligible.

Given that viscosity does not depend on n, one of the major differences between continuum and free molecular considerations is that the electrical mobility of charged particles is independent of n in the continuum regime but inversely proportional to it in the free molecular regime. The necessity of reconciling the two behaviors via a smooth transition requires a parameter that compares size to concentration leading naturally and once again to the appearance of the Knudsen number:

$$Kn = \frac{2\lambda}{d_p} = \frac{2}{n\sqrt{2}\pi d_g^2 d_p} = \frac{1}{3\sqrt{2}N_A}\frac{V_m}{V_g}\frac{d_g}{d_p},$$

Here d_g is the gas molecule diameter, λ is the mean free path, V_g is the gas molecule volume (assuming it is spherical), N_A is Avogadro's number, and V_m is the gas molar volume. The last Kn definition, although

not generally used, suggests a dependence of electrical mobility on the rarefaction (V_m/V_g) of the gas as well as on the ratio of gas size to particle size (d_g/d_p), with the particle itself being a plausible perturbing agent to the flow. Regardless of the obvious necessity, no one general theoretical formula exists that unequivocally captures the evolution of mobility through the different regimes. The reason is most likely that the Knudsen number is not the optimal physical quantity to use, despite the obvious influence, given that V_m, and consequently λ, is not necessarily constant near the charged particle. For example, on one hand, in the free molecular regime, direct interactions of individual gas molecules with the charged particle (or ion) are the prevalent cause of momentum transfer, making the electrical mobility inversely proportional to the collision cross-section of the particle and the gas number concentration. Within the continuum creeping flow, on the other hand, the particle perturbs the gas surrounding the charged particle causing it to be compressed and rarified, leading to the mobility being inversely proportional to a blurred characteristic size (direct impingements on the surface are not as prevalent and have a lower contribution to the drag) and the viscosity of the gas. Therefore, the physical evolution between the two regimes should be trying to account for how secondary gas to gas collisions -collisions that occur between incoming gas molecules and those reflected from the surface that perturb the gas- affect momentum transfer (or equivalently affect the viscosity or mean free path), something not simple by any means.

There have been many attempts to provide estimates to the electrical mobility over the full Knudsen range. Perhaps, the most well-known semi-empirical law describing the mobility of charged particles through the transition regime is known as the Stokes-Millikan equation (although many other names for the same equation do exist)(Robert A Millikan, 1923b):

$$Z_p = \frac{ze}{3\pi\eta(d_p+d_g)}\left\{1+\frac{2\lambda}{d_p+d_g}\left(A_1+A_2\,exp\left[-\frac{A_3(d_p+d_g)}{\lambda}\right]\right)\right\}, \tag{5}$$

where A_i are dimensionless experimentally derived slip factor parameters which depend on the gas. Equation (5) is only meant initially to be used for spherical particles and agrees with the continuum result of eq. (3) for vanishing values of the Knudsen number ($Kn = 2\lambda/(d_p + d_g) \sim 2\lambda/d_p$) and, given an appropriate choice of the A_i values, with diffuse-reflection conditions for the free molecular regime described in eq. (4). The Stokes-Millikan eq. (5) and its derivatives are surprisingly accurate despite the challenges they present. They have been successfully employed in aerosol science(Ehn et al., 2011; Fang et al., 2014; Fernández-García & de la Mora, 2013; Jung, Han, Mulholland, Pui, & Kim, 2013; Ku & de la Mora, 2009), despite not completely satisfying the underlying complicated physics of the phenomena. The fundamental theory leading to the semi-empirical relationship is far from complete and, as new more capable experimental systems are surfacing, it is necessary to revisit our fundamental understanding and offer possible new initiatives to tackle the electrical mobility problem(Hirsikko et al., 2010).

To assist in the above goal, this article offers a review of the approaches used in the field of aerosols to calculate electrical mobility for a charged particle or ion of arbitrary shape and size for low Mach number and electric field strengths. As a comprehensive analysis, it showcases how the flexibility and fluency in which experimental transport properties, such as diffusion or electrical mobility, may be obtained is in contrast with the difficulty required to correctly understand the measured values. The discernment of a comprehensive theory that accurately explains the measurements is nonetheless crucial due to the practical importance of aerosol transport properties in a variety of fields and research disciplines such as nucleation, particle dynamics, atmospheric science, dusty plasmas, material processing, pollution, particle reactors and combustion (Agarwal & Girshick, 2012; Alam & Flagan, 1986; Carbone et al., 2019; Davis, Joshi, Wang, & Egolfopoulos, 2005; Girshick, Chiu, & McMurry, 1990; Girshick & Chiu, 1990; Gopalakrishnan & Hogan Jr, 2012; Kulmala et al., 2013; McMurry, 1983; Pratsinis, 1988; Rogak & Flagan, 1992). Due to the

vast differences in the way the calculation of electrical mobility is handled, one should distinguish between approaches used in the free molecular and transition/continuum regimes, where the former can be handled from an aerosol perspective (momentum transfer approach) rather than using a full kinetic theory approach. Although not addressed in this review, one can access plenty of relevant literature regarding flows at high Mach numbers and/or high electric fields (Bowden & Harbour, 1966; Henderson, 1976; C. Li et al., 2019; Z.-H. Li, Peng, Zhang, & Yang, 2015; Loth, 2008; Edward A. Mason & McDaniel, 1988; McCoy & Cha, 1974; Rose, 1964; Larry A Viehland & Mason, 1975).

Given the broadness of the covered topics, the manuscript is organized in two main discussion sections. Section 2 pertains to the methods used to calculate the value of the electrical mobility of charged particles of spherical shape in the entire range of Knudsen numbers starting from the Stokes solution for the continuum regime. This first section begins with the discussion of the historically relevant and simplest theories (i.e., some variations of the Stokes-Millikan law) before diving into the description of approaches based on more fundamental principles that can be used for refined calculations in the free molecular regimes. The last part of section 2 introduces further corrections of the described methods to include the effect of potential force interactions between the charged particle and the gas molecules and provide the tools to account for the experimentally observed transition from specular to diffuse reflection of the gas molecules at increasing values of the Knudsen number. Section 3 introduces the adaptation of the Stokes-Millikan based methods introduced in the previous section to infer the electrical mobility of particles of arbitrary shape. The results of these modifications are compared to that of more sophisticated and modern approaches, including Monte Carlo simulations, specifically designed to consider particles of any shape in the transitional regime. The last part of Section 3 focuses on the free molecular regime and describes how the most modern modeling tools can be used to perform mobility calculation of entities with specified and detailed atomic structure in which each atom of the structure is the center of an interaction potential with gas molecules. The surveyed literature shows how such types of detailed calculations enable the possibility of predicting the mobility from first principles without performing assumptions on the reflection type of the molecules upon collision with the charged particle. Short final remarks conclude the manuscript content.

2. Mobility Transport Theories for Spherical Particles in the Free Molecular, and Transition Regimes.

2.1 Origins of mobility transport theories for spheres of any size: The Stokes-Millikan equation.

In the low field limit, the first deviations from the continuum regime to account for the effect of the Knudsen number were given by Cunningham using a linear perturbation of the Stokes equation (eqs. 2-3) as(Cunningham, 1910):

$$Z_p = \frac{ze}{3\pi\eta d_p}\left(1 + A\frac{2\lambda}{d_p}\right), \tag{6}$$

with A a constant intended to take into account the law of reflection of the gas molecules upon impingement of the charged particle (slip correction). However, it was made clear that the value of A in eq. (6) had to vary with concentration in the transition region to match experimental results. A semi-empirical formula was then devised by Knudsen and Weber and similarly by Millikan that focused on correctly describing the transition portion (M Knudsen, 1950; Martin Knudsen & Weber, 1911; Robert A Millikan, 1923b). The equation, which appears in the introduction as eq. (5) is labeled Stokes-(Cunningham-Knudsen-Weber)-Millikan equation (in no particular order) and its more primitive version is provided here for convenience:

$$Z_p = ze\frac{1+2\lambda/d_p\left(A+Bexp\left(-\frac{cd_p}{\lambda}\right)\right)}{3\pi\eta d_p} = ze\frac{1+Kn\left(A+Bexp\left(-\frac{2c}{Kn}\right)\right)}{3\pi\eta d_p} \tag{5'}$$

Where A, B and c have the same meaning as the A_i coefficients in eq. (5). The equation agrees with the Stokes equation in the continuum regime and is somewhat reminiscent of the free molecular counterpart (eq. 4) when the Knudsen number approaches infinity. The A_i coefficients have been derived in different ways, for different gases and through different methods, many of them coming from Millikan and his pupils (Derieux, 1918; Eglin, 1923; Ishida, 1923; Lassalle, 1921; Lee, 1914; Silvey, 1916; Stacy, 1923; Van Dyke, 1923). For air, the most commonly used values are given by Davies as $A_1 = 1.257$, $A_2 = 0.4$ and $A_3 = 0.55$ (Davies, 1945). While the first two coefficients are dependent on matching the free molecular expression through the different modes of reflection, the third coefficient, A_3, is empirically adjusted as no theoretical value is known and may vary up to a factor of 2. It is perhaps necessary to explain the values chosen by Davies for the A_i coefficients, as they are not based on theoretical results but rather on averages of previously reported values. Based on results from Millikan, Mattauch, Monch and Knudsen, and Weber (Martin Knudsen & Weber, 1911; Mattauch, 1925; R. Millikan, 1920; Robert A Millikan, 1923a, 1923b; Mönch, 1933), Davies obtains the result for A_1 by averaging the results from the first 3 authors and A_2 using all but Mattauch's results. Lastly, A_3 is obtained through the median of the results from Millikan and Mattauch. While Davies' results are the most commonly used, there are a plethora of published values which seem to vary depending on the particle studied, e.g. solid vs liquid particles. A compilation of slip correction factors appears in Table I (M. Allen & Raabe, 1982; M. D. Allen & Raabe, 1985; Annis, Malinauskas, & Mason, 1972; Buckley & Loyalka, 1989; N. A. Fuchs, Daisley, Fuchs, Davies, & Straumanis, 1965; Metzig, 1984; Rader, 1990; Schmitt, 1959) for air and other gases. Most authors agree on the universality of $A_1 + A_2$ for all gases with a value of approximately ~ 1.65 at standard pressure and temperature.

Table I. Several Slip Correction Factors published in literature for different gases. The values have been modified to reflect a viscosity of $\eta = 0.499 n m_{gas} \lambda \bar{c}$ and standard temperature and pressure. Where only the values of A_1 are reported, consider using Cunnigham's approximation eq. (6) or Rader's extrapolation to obtain A+B.

Source	A_1/A	A_2/B	A_3/c	$A+B/A_1+A_2$	*Surface*	*Gas*
Kudsen and Weber, 1911	1.103	0.572	1.143	1.675	Glass spheres	Air
Millikan, 1923	1.234	0.414	0.876	1.648	Oil-drop	Air
Mattauch, 1925	1.282	0.445	1.66	1.727	Oil drop	N_2
Monch, 1933	1.285				Tobacco Smoke	Air
Davis, 1945	1.257	0.4	1.10	1.657	Derived	Air
Schmitt, 1959	1.45	0.4	0.9	1.85	Silicon droplet	N_2
Annis and Malinauskas, 1972	1.558	0.173	0769	1.731	Predicted	Air
Metzig, 1984	1.2	0.432	1.039	1.632	Solid	Air
Allen and Raabe, 1985	1.142	0.558	0.999	1.700	Solid/PSL/PVT	Air
Buckley and Loyalka, 1988	1.099	0.518	0.425	1.617	Fit to low Kn	Air
Rader, 1989			0.78	1.647	Extrapolated	Air
Ishida, 1923	1.207				Oil-drop	Air
Stacy, 1923	0.983				Machined Brass	Air
Van Dyke, 1923	1.114				Cleaned brass	Air
Ishida, 1923	1.277				Oil-drop	He
Rader, 1989			0.92	1.647	Extrapolated	He
Millikan, 1923	1.144				Oil-drop	H2
Ishida, 1923	1.141				Oil-drop	H2
Ishida, 1923	1.208				Oil-drop	CO2
Eglin, 1923	1.150				Oil-drop	CO2
Lasalle, 1921	1.160				Oil-drop	CO2
Van Dyke, 1923	1.142				Shellac Resin	CO2
Rader, 1989			2.0	1.647	Extrapolated	CO2
Rader, 1989	A_1	1.647-A_1	~0.85	1.647	Extrapolated	All gases

When eq. (5 (or equivalently 5')) is compared to its free molecular counterpart, eq. (4), for $Kn \gg 1$, a relation between CCS and mobility diameter may be inferred. If one assumes that $m_w \gg m_{gas}$ ($m_{red} \sim m_{gas}$), $T_{eff} \sim T$, and that the viscosity is given by $\eta = 0.499 n m_{gas} \lambda \bar{c} = 0.499 n \lambda \sqrt{\frac{8kTm_{gas}}{\pi}}$ (Larriba & Hogan, 2013b), the comparison yields:

$$\bar{\Omega}_{1,1}(T_{eff}) = \frac{9}{4(A_1+A_2)} \frac{\pi}{4} (d_p + d_g)^2 = \frac{9}{4(A_1+A_2)} PA = \xi PA \,, \tag{7}$$

where PA is the equivalent of a Projected Area for a hard sphere of effective diameter $d_p + d_g$ and ξ is the accommodation enhancement factor. As its name suggests, ξ is a measure of the effective increase of the CCS over PA due to momentum accommodation, i.e. how the momentum transfer is adjusted due to gas molecule-particle hard sphere interaction upon a collision. If the results from Davies are applied to eq. (7), it yields a value $\xi = 1.3578$. As will be later derived, the value of ~1.36 is assumed to be caused by a predominantly diffuse reflection of the gas molecules after impingement on the surface (Epstein, 1924). The diffuse reflection explanation is extensively used although its elusive theoretical justification is a subject of enormous debate, and not without reasons. In principle, the expectation is that molecular collisions should eventually become more specular as the size of the charged particle becomes sufficiently small (which will also be shown to yield $\xi \sim 1$) contradicting the asymptotic results to the Stokes-Millikan (Z. Li & Wang, 2003a, 2003b; Tammet, 1995). This would suggest that an evolution from specular to diffuse must take place within the free molecular regime, something not accounted for in Stokes-Millikan. To properly understand the results behind eq. (7), a more rigorous introduction of the theory of electrical mobility in the free molecular regime is necessary and provided in section 2.2.

One must also reflect here on the meaning of the mobility diameter d_p. Given that most aerosol particles are not perfectly spherical, d_p does not normally describe the physical diameter of the particle but rather a measure of the mobility of the particle. It should not be compared to a physical mass diameter unless the charged particle is spherical, of a known density, and the effects of interaction potentials are negligible or very well quantifiable. The non-spherical effects are addressed in section 3.

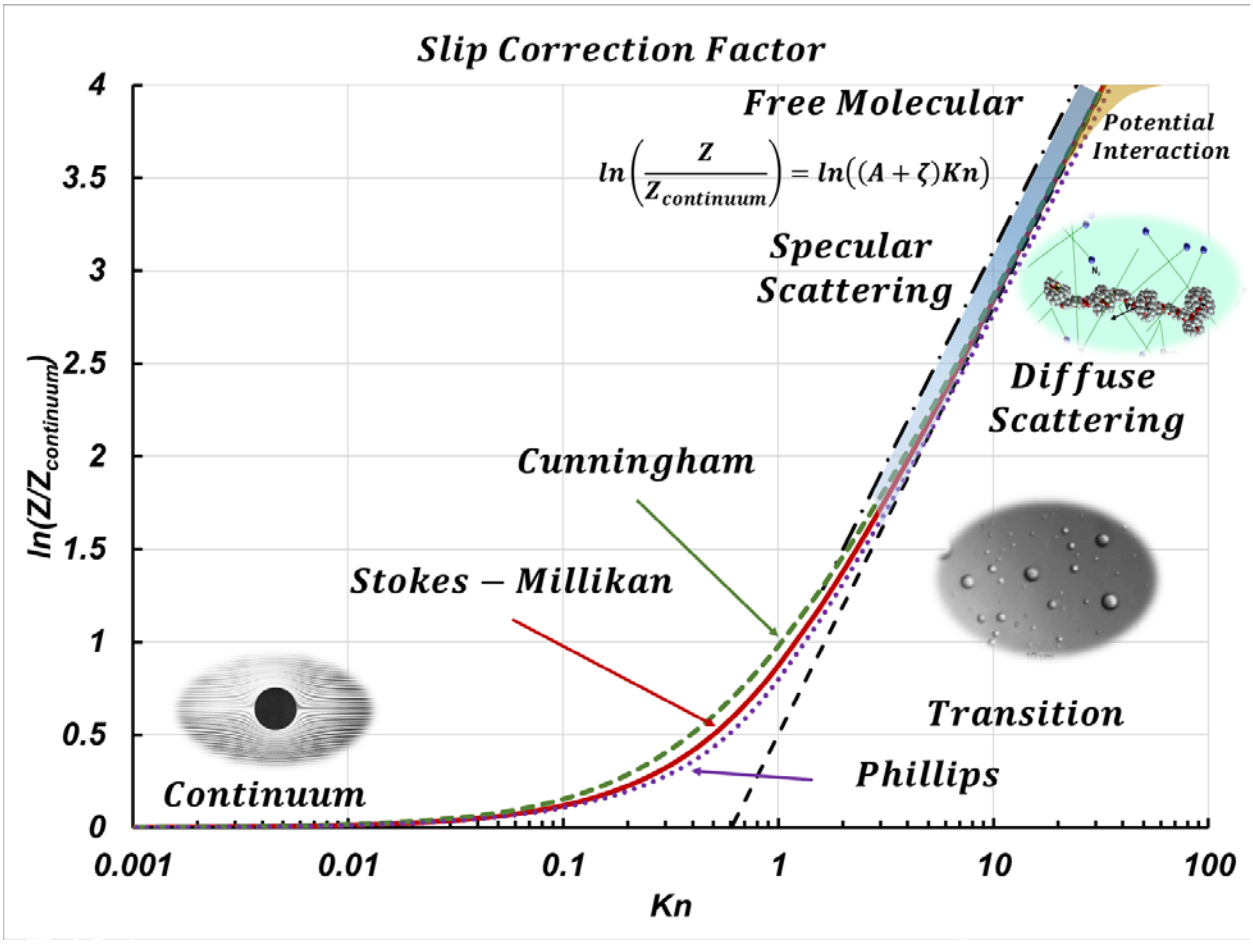

Figure 2. Mobility as a function of Knudsen numbers from continuum to free molecular regimes showing Stokes-Millikan, Cunningham, and Phillips approximations. On the free molecular portion, approximations for diffuse and specular scattering are represented.

It is perhaps beneficial at this point to highlight the existence of other mobility calculations that encompass the free molecular and continuum regimes but do not rely directly on the Stokes-Millikan equation. As an example, these include Basset's solution to the continuum equations with slip boundary conditions (Basset, 1888) and Goldberg's as well as Liu and Sugimura's approximate solution to moments of the Boltzmann equation (Goldberg, 1954; C. Liu & Sugimura, 1969; Sugimura, 1968). Perhaps the most used form is that of Phillips who solves an approximation to six moments of the Boltzmann equation while matching the behavior of both continuum and free molecular regimes (Phillips, 1975):

$$Z_p = \frac{ze}{3\pi\eta d_p}\frac{5+4c_1Kn+3(c_1^2+1)Kn^2+6(c_2(c_1^2+2)Kn^3}{5-c_1Kn+c_2(8+\pi)(c_1^2+2)Kn^2/3} \quad ;c_1 = \frac{2-\alpha}{\alpha} \quad ;c_2 = \frac{1}{2-\alpha} \qquad (5'')$$

with α being the percentage of molecules that have been thermally accommodated and which Phillips himself set to 0.895 guided by Millikan's work (Robert Andrews Millikan, 1911; Robert A Millikan,

1923b). The expression from Phillips reproduces the results from Millikan's oil drop experiments to within 2%.

Figure 2 captures the variation of electrical mobility from continuum to free molecular as a function of the Knudsen number for a spherical charged particle. The estimations from Cunningham (eq. 6), Stokes-Millikan (eq. 5) and Phillips (eq. 5'') are plotted showing the validity of all the approximations to predict the full range of values. The results from eq. (4) are also plotted for the free molecular regime with $\xi \sim 1.36$ for diffuse reflection and $\xi = 1$ for specular reflection. Note how Cunningham's eq. (6) is sufficient to correctly approximate, at least asymptotically, the free molecular regime for diffuse reflection when A is taken to be 1.657. Hence eq. (6) may be used to provide a simple asymptotic equation for the free molecular as presented in the figure, with the ζ variable being a function of the Knudsen number. The blue shaded area in Figure 2 shows how an appropriate choice of ζcould potentially yield values anywhere between the specular and diffuse reflection scattering asymptotes. The diffuse and specular scattering limits depicted in Figure 2 may be considered to be bounds to the calculation at least until the interaction potentials become non-negligible (around 2nm for singly charged particles). Potential interactions are difficult to characterize due to their dependence on the charge and polarizability of the charge. They can be represented by the yellow shaded area Fig 2.

2.2 Calculations of electrical mobility in the Free Molecular Regime.

As noted in the previous section, in order to understand how diffuse/specular collisions affect mobility in the free molecular regime, one must provide a comprehensive examination of how the drag force may be calculated in a deterministic fashion. The study of transport properties in the free molecular regime dates back to Chapman and Enskog and their study of diffusion (Chapman & Cowling, 1970), and where the analysis of electrical mobility appears from its close connection with diffusion through Einstein's relation (Einstein, 1905; Smoluchowski, 1906). Upon the difficulty that studying the interaction between gas and charged particle entails, some general assumptions must be considered prior to providing a suitable transport equation for the charged particle. The first, and probably most important, is that the charged particle or ion (perhaps a more accurate description within the free molecular regime) does not perturb the buffer gas, and thus every interaction of gas molecule with the charged particle is independent of the rest (Kihara, 1953). This allows for the gas velocity to assume a three-dimensional Boltzmann distribution:

$$f(c_i) = \left(\frac{m_{gas}}{2\pi kT}\right)^{\frac{3}{2}} \exp\left(-\frac{m_{gas}c^2}{2kT}\right), \tag{8}$$

with $c^2 = c_1^2 + c_2^2 + c_3^2 = c_i c_i$ the square of the gas thermal velocity magnitude, and c_i being any ith coordinate of such velocity.

The ion velocity distribution cannot be readily defined unless certain approximations are first established. The reason is that the distribution is dependent on the external contribution of the field and hence a Boltzmann equation for the distribution must be first constructed. Assuming that the charged particle concentration is much smaller than the concentration of gas molecules as well as small enough so that charged particles do not interact with each other, a viable collision operator for the Boltzmann equation can be inferred. Using this collision operator, a solution of the first few moments of the Boltzmann equation can be attempted, including the drift velocity and hence the electrical mobility (Edward A. Mason & McDaniel, 1988; Edward A Mason & Schamp Jr, 1958). This procedure is known as the kinetic theory approach. However, discussing the moments of the Boltzmann equation is beyond the scope of this review, but the solution to approximations of the first few moments have been provided by Kihara, Mason and Schamp and Viehland among others (Kihara, 1953; E. Mason & Hahn, 1972; Edward A. Mason &

McDaniel, 1988; Edward A Mason & Schamp Jr, 1958; Larry A Viehland & Mason, 1975, 1978). For the two-temperature theory, the first approximation to drift velocity moment leads to eq. (4) where the first collision integral, or CCS, can be written from momentum transfer considerations in the form of a quadrature:

$$\bar{\Omega}_{Teff}(1,1) = \frac{1}{8\pi^2}\int_0^{2\pi}\int_0^{\pi} sin\phi \int_0^{2\pi}\int_0^{\infty} g^{*5} e^{-g^{*2}} dg^* \int_0^{\infty} 2\pi b\left(1-\cos\left(\chi_{def}\right)\right) db\, d\theta d\phi d\gamma \qquad (9)$$

where ϕ, θ and γ are the ion orientation angles with respect to the incoming gas molecules, g^* is a dimensionless relative velocity between ion and gas molecule, b is the impact parameter, and χ_{def} is the resulting deflection angle of the gas molecule due to the interaction with the particle. The most interesting feature in this equation is that the quadrature can be analytically calculated if the deflection angle χ_{def} is known. However, due to the intricate relations that affect the deflection angle, including potential interactions, inelastic collisions, and scattering effects, this angle is generally calculated numerically under most circumstances. Nonetheless, the deflection angle may be calculated analytically for relatively simple and convex geometries, e.g. spherical, as long as the potential interactions are negligible or their contribution can be accounted for, e.g. a central force. It should be noted here that when the CCS is averaged over all orientations in eq. (9), drift velocity, drag, and electric field have been assumed to be in the same direction, a simplification that works well for small ions but does not necessarily have to be true in principle. Finally, higher-order approximations to the Mason-Schamp equation do exist, but the error committed for using the first approximation is minimal for most if not all aerosol particles and small fields/Mach numbers (Larry A Viehland & Mason, 1975, 1978; L. A. Viehland & Mason, 1995).

Despite the success of the solution to the moments' method (kinetic theory approach), a different approach more akin to aerosol science and focusing on direct momentum transfer is provided here (Epstein, 1924). The consideration of this slightly different approach is based mainly on two reasons. The first consideration comes from the realization that solving eq. (9) when hard sphere interactions are considered, yields $\bar{\Omega}_{Teff}(1,1) = \frac{\pi}{4}\left(d_p + d_g\right)^2 = 1 * PA$, akin to specular and elastic interactions, which would be insufficient to predict the necessary drag to match the experimental results provided by Millikan using oil drops, as was established in eq. (7). It appears that a modification of the particle collision model is necessary to reproduce the asymptotic behavior of the Stokes-Millikan equation. One simple modification to achieve this result considers the possibility that a fraction of all impinging gas molecules is subject to inelastic and diffuse collisions. The second consideration is that, given that aerosols are seldom highly charged and have masses much larger than gas molecules, the reduced mass and potential interaction effects may be safely ignored under most scenarios. This second relaxation, as stated above, allows for analytical calculations to be performed when the particle may be considered convex and not excessively complicated (Fernández de la Mora, 2002; Garcia-Ybarra & Rosner, 1989; Ivanov & Yanshin, 1980), so a more suitable expression based on the wetted surface area of the ion would be preferred. As a result of these considerations, a simplified calculation focusing on convex particles with inelastic collisions was the most logical approach to deal with aerosols. For the sake of completeness, it should be noted that inelastic approaches to polyatomic systems are indeed possible within the kinetic theory approach as well. The so-called Wang Chang-Uhlenbeck-de Boer (WUB) equation is akin to the Boltzmann equation but allows for a semi-classical approach where internal states of both gas molecules and charged particles may change after a collision (Chang, Uhlenbeck, & de Boer, 1964; Monchick, Pereira, & Mason, 1965; Monchick, Yun, & Mason, 1963).

It is customarily acceptable to assume a solution to the Boltzmann equation by providing a guess to the charged particle velocity distribution. It can be shown that, for a vanishingly small electric field to

concentration ratio, E/n~0, and sufficiently massive ions ($m_w > 4m_{gas}$) (Kihara, 1953; Edward A Mason & Schamp Jr, 1958), the velocity distribution of a charged particle or ion drifting with velocity v_{d_i} may be given by:

$$F(z_i) = \left(\frac{m_w}{2\pi kT}\right)^{3/2} \exp\left(-\frac{m_w(z_i - v_{d_i})^2}{2kT}\right) \tag{10}$$

with z_i the indexed velocity of a charged particle and where $(z_i - v_{d_i})^2$ is understood as the square of the magnitude of the resulting vector difference. By means of eqs. (8) and (10), one can proceed to calculate the drag force by calculating the excess momentum transfer of gas molecules colliding with the drifting ion. Such calculation was attempted initially by Langevin and Cunningham assuming only specular and elastic collisions (Cunningham, 1910; Langevin, 1905), expanded by Lenard and completed by Epstein both of whom assumed other cases of reflection (Epstein, 1924; Lenard, Weick, & Mayer, 1920). For the sake of generality and agreement with the analytical chemistry field, the calculations carried out here differ slightly from those of previous authors. The reason is that in order to consider reduced masses, both the gas and ion velocity distributions (eqs. 8 and 10) must be taken into account, as opposed to Epstein's approach who directly assumed that the aerosol mass is much greater than that of the gas molecule, indirectly neglecting the reduced mass effects. The end result however qualitatively agrees with that of Epstein and other authors such as Waldmann (Waldmann, 1959).

To calculate the momentum transfer of gas molecules onto the charged particle, it is customary to initially calculate the number of gas molecules per unit time colliding onto an infinitesimal surface of the particle $d\Sigma$ (which maybe expanded to include the diameter of the gas) with normal n_i and integrating over the whole surface (dropping the dependencies of the distributions f and F):

$$Q = n \oint \int \quad \int \quad fFg_i \cdot n_i|_{g_i \cdot n_i < 0} d^3c_i d^3z_i \, d\Sigma,$$

where $g_i = z_i - c_i$ is the relative velocity of the gas molecules impinging on the ion's surface and the condition $g_i \cdot n_i < 0$ represents that only gas molecules incoming from the outside of the particle are counted. d^3c_i and d^3z_i represent the integration over all three components, e.g. $dc_1 dc_2 dc_3$.

To account for inelastic collisions, the momentum transfer is separated between impinging and reflected molecules. The momentum transfer per unit time of the impinging gas molecules, $\dot{p}_j^-$ can be obtained straightforwardly by multiplying the flux of impinging molecules by their momentum $m_{gas}c_j$:

$$\dot{p}_j^- = n \oint \int \quad \int \quad fFm_{gas}c_j g_i \cdot n_i|_{g_i \cdot n_i < 0} d^3c_i d^3z_i \, d\Sigma \tag{11}$$

To make the calculation a little more tractable, a change of variables is performed from world variables c_i and z_i to relative velocity and the center of mass velocity (Kruger & Vincenti, 1965):

$$W_i = \frac{m_{gas}c_i + m_w z_i}{m_{gas} + m_w}$$

Given that $d^3c_i d^3z_i = d^3W_i d^3g_i$, one can then integrate the equations over the center of mass velocity yielding:

$$\dot{p}_j^- = n\left(\frac{m_{red}}{2\pi kT}\right)^{3/2} \oint \int \quad e^{-\frac{m_{red}(g_i - v_{d_i})^2}{2kT}} m_{red} g_j g_i \cdot n_i|_{g_i \cdot n_i < 0} d^3g_i \, d\Sigma \tag{12}$$

Under the assumptions of low electric field and large masses, $v_{di} \ll g_i$, the exponential may be linearized taking only the first two terms of the expansion to yield some useful analytical relationships:

$$\dot{p}_j^- = n\left(\frac{m_{red}}{2\pi kT}\right)^{3/2} \oint\int \quad e^{-\frac{m_{red}g^2}{2kT}}\left(1 - \frac{2m_{red}}{2kT} g_i \cdot v_{d_i} + \cdots\right) m_{red} g_j g_i \cdot n_i|_{g_i \cdot n_i < 0} d^3 g_i \, d\Sigma \quad (13)$$

Although it may seem at first that the linearization is unnecessary, it allows for an analytical separation between the unperturbed (the unit term) flow and its perturbation ($\frac{2m_{red}}{2kT} g_i \cdot v_{d_i}$). This becomes quite important for convergence, as the total momentum transfer of the unperturbed flow is 0 and can be removed from the analysis. It can also be used to show that the drag force and electric field are not assumed to be in the same direction as the drift velocity.

One can now integrate eq. (13) over all relative velocities. It is customary to separate the result into surface normal and surface tangential projections and, assuming without loss of generality that $g_1 = g_i \cdot n_i$, $g_2 = g_i \cdot t_{1i}$ and $g_3 = g_i \cdot t_{2i}$, the result for impinging momentum transfer yields:

$$\dot{p}_j^- = -nm_{red}\sqrt{\frac{m_{red}}{2\pi kT}} \oint\int \quad \left(\frac{1}{4}\sqrt{\frac{\pi m_{red}}{2kT}} + v_{d_i} \cdot n_i\right) n_j + \frac{1}{2}\left(v_{d_i} \cdot t_{1i}\right) t_{1j} + \frac{1}{2}\left(v_{d_i} \cdot t_{2i}\right) t_{2j} d\Sigma \qquad (14)$$

For the reflected gas molecules, one has to choose whether they are reemitted specularly or diffusely and whether elastically or inelastically. Let us assume for now that a mixture of the two cases exists. For those molecules reflected diffusely, let us also assume that the gas molecules become thermally "accommodated" to the particle temperature before leaving the surface in a random direction. If the accommodation coefficient α represents the fraction of reflected gas molecules that leave the surface at the surface temperature, the momentum transfer of that fraction $\dot{p}_{dif}^+$ is given by:

$$\dot{p}_{dif_j}^+ = n_\alpha \left(\frac{m_{red}}{2\pi kT}\right)^{3/2} \oint\int \quad e^{-\frac{m_{red}g^2}{2kT}} m_{red} g_j g_i \cdot n_i|_{g_i \cdot n_i > 0} dg_i \, d\Sigma, \qquad (15)$$

where n_α is the number concentration of gas molecules reemitted diffusively and the condition $g_i \cdot n_i > 0$ now refers to the gas molecules leaving the surface. The n_α fraction is given by equating the fraction of the impinging flux that will become accommodated to the equivalent reflected flux. Calculating the fraction of the flux of particles that collide with a surface differential per unit time yields:

$$Q_{\alpha-} = \alpha n \oint\int \quad e^{-\frac{m_{red}g^2}{2kT}}\left(1 - \frac{2m_{red}}{2kT} g_i \cdot v_{d_i}\right) g_i \cdot n_i|_{g_i \cdot n_i < 0} dg_i d\Sigma = \oint \frac{\alpha n}{2}\left(\sqrt{\frac{2kT}{\pi m_{red}}} + v_{d_i} \cdot n_i\right) d\Sigma \qquad (16)$$

This result must be equal to the number of particles that leave the surface diffusely per unite time (with $g_i \cdot n_i = g_1$):

$$Q_{\alpha+} = n_\alpha \oint\int \quad e^{-\frac{m_{red}g^2}{2kT}} g_i \cdot n_i|_{g_i \cdot n_i > 0} dg_i d\Sigma = \oint \frac{n_\alpha}{2}\sqrt{\frac{2kT}{\pi m_{red}}} d\Sigma. \qquad (17)$$

Comparing integrands yields between eqs. (16) and (17):

$$n_\alpha = \alpha n\left(1 + \sqrt{\frac{\pi m_{red}}{2kT}} v_{d_i} \cdot n_i\right) \qquad (18)$$

Now, one is in a position to calculate the momentum transfer of the molecules that undergo diffuse reflections. Using eqs. (15) and (18):

$$\dot{p}^{+}_{dif_j} = \frac{\alpha n m_{red}}{4}\sqrt{\frac{2\pi kT}{m_{red}}}\oint\left(\sqrt{\frac{2kT}{\pi m_{red}}} + v_{d_i}\cdot n_i\right)n_j d\Sigma \tag{19}$$

The rest of the reflected gas molecules, $1-\alpha$, are assumed to be emitted specularly. After the reflection, the relative velocity will be given by $g_j - 2(g_i\cdot n_i)n_j$ so that the momentum transfer is given by:

$$\dot{p}^{+}_{spc_j} = (1-\alpha)n\left(\frac{m_{red}}{2\pi kT}\right)^{3/2}\oint\int\ e^{-\frac{m_{red}g^2}{2kT}}\left(1-\frac{2m_{red}}{2kT}g_i\cdot v_{d_i}\right)m_{red}g_j - 2(g_i\cdot n_i)n_j g_i\cdot n_i|_{g_i\cdot n_i<0}dg_i\,d\Sigma, \tag{20}$$

which if integrated yields:

$$\dot{p}^{+}_{spc_j} = (1-\alpha)\left(-\dot{p}^{-}_{i}\cdot n_i n_j + \dot{p}^{-}_{i}\cdot t_{1i}t_{1j} + \dot{p}^{-}_{i}\cdot t_{2i}t_{2j}\right) \tag{21}$$

The difference between the momentum transfer of the reflected and impinging gas molecules yields the total drag:

$$F_{D_j} = \dot{p}^{+}_{dif_j} + \dot{p}^{+}_{spc_j} - \dot{p}^{-}_{j} = 2nm_{red}\sqrt{\frac{2kT}{\pi m_{red}}}\oint\left[\left(1-\frac{\alpha}{2}+\frac{\alpha\pi}{8}\right)n_i n_j + \frac{\alpha}{4}\left(t_{1i}t_{1j}+t_{2i}t_{2j}\right)\right]\cdot v_{d_i}\,d\Sigma \tag{22}$$

Adding and subtracting $\frac{\alpha}{4}n_i n_j$ and realizing that $n_i n_j + t_{1i}t_{1j} + t_{2i}t_{2j} = \bar{\bar{I}}$ leads to (Fernández de la Mora, 2002):

$$F_{D_j} = \left\{2nm_{red}\sqrt{\frac{2kT}{\pi m_{red}}}\oint\left[\left(1-\frac{3\alpha}{4}+\frac{\alpha\pi}{8}\right)\overline{\overline{nn}} + \frac{\alpha}{4}\bar{\bar{I}}\right]d\Sigma\right\}\cdot v_{d_i} \tag{23}$$

Eq. (23) is the standard drag force expression for charged particles. After integration over the wettable surface area of the particle (Σ), a drag tensor B_{ij} may be obtained (bracketed in eq. 23), which, when multiplied by the drift velocity, will yield the drag force for a particular orientation of the charged particle:

$$F_{D_j} = B_{ij}v_{d_i};\quad with\ F_{D_j} = zeE_j \tag{24}$$

As expected, eq. (24) allows for the drag force and the drift velocity to be in different directions. To be able to obtain a single value for mobility from eq. (24) instead of a tensorial expression, one has to make an assumption about the orientation of the particle subject to the electric field. If all orientations are assumed to be equally probable, an average value may be obtained. A difficulty that arises is whether the drag tensor or its inverse should be calculated to obtain a metric of the mobility that may be compared to experiments. There has been much controversy surrounding the correct averaging. Based on results from Landau and Lifshitz and (Landau & Lifshitz, 1975), later on, Happel and Brenner (Happel & Brenner, 2012), the mobility was primarily averaged using the inverse of the tensor so that, once the tensor was diagonalized using the principal directions, the mobility would be given by:

$$Z_{pH\&B} = \frac{ze}{3}\left(\frac{1}{B_{11}}+\frac{1}{B_{22}}+\frac{1}{B_{33}}\right) \tag{25}$$

However, the result of the mobility using eq. (25) does not agree with the results from Mason & Schamp in eq. (4) even for specular collisions unless the charged particle meets certain criteria, e.g. being spherical. Upon revision of the results from Happel and Brenner, however, it is clear that the displacement per unit time they calculated was in the direction of the "settling velocity" (here called drift velocity) and not its component in the direction of the drag or electric field, being the latter projection the only magnitude that can be measured by an instrument. Hence the result from eq. 25 should not be compared to experimental results (Carlos Larriba-Andaluz, Nahin, & Shrivastav, 2017). Conversely, performing the average of the drag tensor rather than its inverse gives the average displacement in the direction of field and has been

shown to agree exactly with the results from Mason and McDaniel (Carlos Larriba-Andaluz et al., 2017), so that:

$$Z_p = \frac{3ze}{(B_{11}+B_{22}+B_{33})} \tag{26}$$

should be used when the electrical mobility is calculated in the free molecular regime under the assumption of all orientations being equally probable. Some authors have estipulated that the applicability eq. (26) (or seemingly eq. 4) relies on the assumption that it is only valid in the fast rotation limit of a small ion(M. Li, Mulholland, & Zachariah, 2014). However, given that no assumption regarding the speed of rotation of the charged particle was ever provided in the analysis of Mason & Schamp (Edward A Mason & Schamp Jr, 1958), nor is it required to arrive at the results of eq. (4), this explanation cannot convey a rigorous physical portrayal of the phenomenon and should be re-examined. In all, Eq. (25) is not incorrect, and, in fact, its results provide what may be regarded as the "true mobility" of the particle (Carlos Larriba-Andaluz et al., 2017), to differentiate it from the "projected mobility" in the direction of the field. For example, two particles with drastically different "true mobility" may be indistinguishable from each other in an instrument because their projected displacement per unti time in the direction of the field is the same(Carlos Larriba-Andaluz et al., 2017). A final note is that eq. (25) may still be used benefitting from the fact that for most globular ions, the difference between eq. (25) and (26) is only a few percent. However, this difference becomes substantially larger for particles of high aspect ratios.

Eqs (26) and (4) will yield identical results as long as the CCS is calculated in an analogous form to how momentum transfer is considered for eq. (26), i.e. hard sphere interactions only. To understand the effects of inelastic vs. elastic or diffuse vs. specular collisions, it is customary to use a sphere as the charged particle. However, the use of a sphere neglects secondary scattering effects of gas molecules colliding more than once with the charged particle, which may increase the overall drag force. Equation (23) for a sphere may be reduced, after integrating, to:

$$F_{D_j} = \frac{16}{3} n \sqrt{\frac{kTm_{red}}{2\pi}} \left(1 + \frac{\alpha\pi}{8}\right) PA \cdot v_{d\,i} = \frac{16}{3} n \sqrt{\frac{kTm_{red}}{2\pi}}\, \bar{\Omega}_{1,1} \cdot v_{d\,i}, \tag{23'}$$

where $\bar{\Omega}_{1,1} = \left(1 + \frac{\alpha\pi}{8}\right) PA = \xi PA$ by means of comparing eqs. (23'), (26) and (4). One can now attempt to understand the result conveyed by eq. (7), i.e. $\Omega = \xi PA \sim 1.36PA$ for a hard-spherical entity with no potential interactions. Different choices of α or different reemission laws would provide different values of ξ. The issue at hand is that the exact reflection law is unknown so an informed guess of how the reemission occurs must be suggested to match the empirical evidence. Three different scenarios will be assumed for the reflecting molecules; elastic/specular, elastic/diffuse, and inelastic/diffuse with full accommodation at the surface temperature. Many other reflection cases have been studied, however, as shown by Epstein, many of them violate thermodynamic principles and are only shown for historical reasons (Epstein, 1924). A representation of the most significant gas-particle interactions used in literature are given in Figure 3. If all collisions are assumed to be specular and elastic, as depicted in Figure 3A, the value of the accommodation coefficient α must be set to 0. This yields a value of $\xi = 1$, which is about 36% off the expected Stokes-Millikan value. On the other hand, if one considers only inelastic diffuse with full accommodation, as shown in Figure 3B, $\alpha = 1$ and the value of ξ increases to $\xi = 1 + \pi/8 = 1.3927$, a value very close to the one using the slip coefficients from Davies. If reflections are assumed to be elastic and diffuse, which would require a small modification of the equations presented here, it would yield $\xi = 1.4445$. In order to match the value provided by Millikan in eq. (7), Epstein hypothesized that one tenth of the molecules should be reflected specularly while the rest would have a diffuse inelastic reflection with

full accommodation to the surface temperature, yielding the very common value used nowadays of $\xi = 1 + \alpha\pi/8 = 1.3574$ with $\alpha = 0.91$.

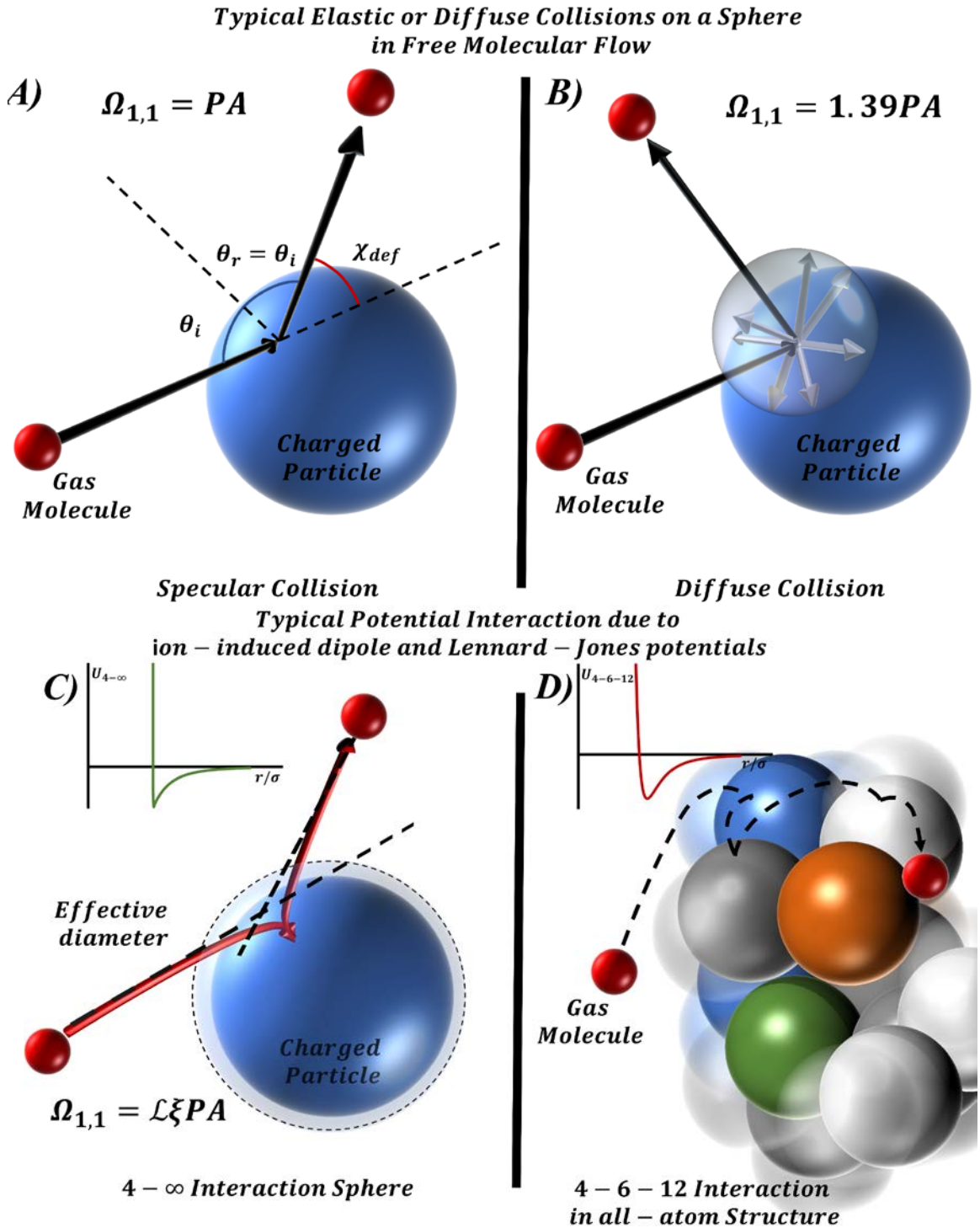

Figure 3. Different possible gas-molecule particle interactions, including specular and diffuse as well as potential interactions. A) Specular reemission. B) Diffuse Reemission. C) $4-\infty$ interaction. D) 4-6-12 interaction with subunits of the particle.

Based on the results from Epstein and Millikan, Friedlander and Fernandez de la Mora employed similar expressions for the scattering based on the accommodation coefficient $\xi = (1 + \alpha\pi/8)$ and they showed

that under most scenarios $\alpha = 0.91$ yields a more than reasonable result for most of singly charged particles down to ~2nm at least in air (de la Mora, De Juan, Liedtke, & Schmidt-Ott, 2003; Friedlander, 2000). The value of 0.91 is however an asymptotical result at best and fails to explain the mostly specular behavior observed for very small ions, in particular when they are drifting in light monoatomic gases such as He (Gotts, von Helden, & Bowers, 1995; Z. Li & Wang, 2003b; Tammet, 1995). Undoubtedly, the value of α is a subject of tremendous debate for numerous reasons. The seemingly artificial choice of 91% inelastic diffuse and 9% elastic specular is the first of such issues. While it may seem like a reasonable choice for an ideal sphere, its applicability may be questioned for entities with resolved atomic structure and non-spherical particles. How the transition occurs from diffuse to specular as the Knudsen number is increased is also incredibly hard to assess. One of the main reasons is the complexity of the rationale behind the diffuse nature of the collisions, a problem accentuated by the fact that the cause seems to differ from one substance-gas pair to another (B. E. Dahneke, 1973b; Phillips, 1975), having no universality on how the collisions migrate towards becoming more specular. Given the variability of the accommodation coefficient α and its empirical nature, its use should be steered mostly towards calculations for charged particles approaching the transition regime and should not be trusted for very small ions (smaller than ~3nm at atmospheric pressure). Perhaps a very good discussion on the nature of specular to diffuse effects is given by Li and Wang (Z. Li & Wang, 2003a, 2003b). Given that a more precise calculation, one that includes entities with resolved atomic structure and potential interactions, must be provided in order to better understand how the specular to diffuse transition occurs, the discussion shall be continued when dealing with non-spherical particles below in Section 3.

A final point that needs to be addressed is the lack of any potential interaction in the treatment of eq. (23). The longest potential interaction to consider is that regarding the induced-dipole potential. While this potential interaction is negligible for singly charged particles with diameters over 2nm (Larriba et al., 2011), it could easily represent increases in the CCS of over 200% for small ions and heavily charged entities (Canzani, Laszlo, & Bush, 2018; Fernández-García & de la Mora, 2014; Ku & de la Mora, 2009; Hui Ouyang, Larriba-Andaluz, Oberreit, & Hogan Jr, 2013) in air or nitrogen, and has been shown to be critical in nucleation and new particle formation (Gamero-Castano & de la Mora, 2002; Iida et al., 2006; Kusaka, Wang, & Seinfeld, 1995; Laakso, Mäkelä, Pirjola, & Kulmala, 2002). While potential interactions will be addressed more carefully for non-spherical particles, most simple potential interactions can be accounted for in the case of spherical charged particles through numerical integration of the deflection angle in eq. (9). For example, for any central force with potential interaction $\Phi(R)$, the quadrature to calculate the deflection angle is given by (Kruger & Vincenti, 1965):

$$\chi_{def} = \pi - 2\int_{\infty}^{R_0} \frac{bdR}{R^2\left[1-\frac{b^2}{R^2}-\frac{\Phi(R)}{\frac{m_{red}g^2}{2}}\right]} \tag{27}$$

where R is the distance between force center and gas molecule and R_0 is the apsidal distance. Overall, the effect of this type of interaction potential can be regarded as an increase in the particle diameter. As such the effective diameter may be calculated as:

$$d_{p,eff} = d_p\left[1-\frac{2\Phi(d_p)}{g^2 m_{red}}\right]^{1/2} \tag{28}$$

Eq. (28) suggests for an additional parameter that modifies the CCS value to account for a potential interaction so that $\overline{\Omega}_{1,1}(T_{eff}) = \mathcal{L}\xi PA$, and where $\mathcal{L}$ lumps the effect of the potential interactions which could be loosely related to $\left[1-\frac{2\Phi(d_p)}{g^2 m_{red}}\right]^{1/2}$ but can also be expanded to accommodate non-spherical

particles with multiple charge locations. Figure 3C shows the typical effect of a central force interaction between gas molecule and charge as an ion-induced dipole interaction and a hard sphere, labeled as a $4-\infty$ interaction, and where the outcome, in this case, may be regarded as an increased effective diameter. Many other potential interactions may be added. As an example, Figure 3D shows a 4-6-12 soft interaction, when dispersive attraction forces are incorporated by the sixth power law exponent, and where repulsion is no longer considered to be infinite but is substituted by a repulsive twelfth power law. However, such complex interactions are better implemented in entities with resolved atomic structure or coarse-grained structures, where the contributions of different elements may lead to an effectively diffuse interaction as shown in the following sections. From all these considerations, it is clear that further corrections to the Stokes-Millikan equation must be required when approaching the free-molecular regime.

2.3. Further corrections to the Stokes-Millikan Equation

With the knowledge acquired from free molecular regime considerations, one can envision certain modifications of the Stokes-Millikan equation to understand the theoretical nature of its empirical parameters and to improve its predictive capabilities. Indeed, there are a plethora of different kinetic theory approaches, with some of them being inconsistent (N. Fuchs, Stechkina, & Starosselskii, 1962), which can give more insight into the electrical mobility problem. The most rigorous treatments involve attempts at solving the Boltzmann equation or the Bhatnagar-Gross-Krook simplification of it (BGK)(V. C. Liu, Pang, & Jew, 1965; Pao & Willis, 1969). Cercignani et al. developed a calculation based on the BGK model that is valid for all Knudsen numbers and axisymmetric bodies (C Cercignani & Pagani, 1968; CDCDP Cercignani, Pagani, & Bassanini, 1968). The variational procedure is quite cumbersome, but the results closely resemble those of Millikan (eq. (5')). One interesting result is that of Annis et al. which is based loosely on kinetic theory (Annis, 1971; Annis et al., 1972). They assume that the motion of the particle can be described as a combination of a viscous and a diffusive component so that:

$$v_d = v_{d_{viscous}} + v_{d_{diffuse}} = \frac{zeE}{3\pi\eta d_p} + \frac{zeE(n+N)D}{p}, \tag{29}$$

where N is the number concentration of charged particles, $p = nkT$ is the gas pressure, and D is the diffusion coefficient. From the drift velocity, the electrical mobility may then be expressed as:

$$Z_p = ze\frac{kT+\frac{(n+N)}{n}3\pi\eta d_p D}{3\pi\eta d_p kT}, \tag{30}$$

which resembles Cunningham's approach in eq. (6). The kinetic theory portion comes from the determination of the diffusion coefficient using Chapman-Enskog's approximation. Rather than just the free molecular approximation to diffusion, there must be an additional effect due to the extra pressure that appears when leaving the free molecular regime. As such:

$$D = \frac{[D]_1}{1-\Delta} \tag{31}$$

where $[D]_1$ is the first approximation to the diffusion coefficient in the free molecular regime and Δ includes the correction from the change in pressure (Hirschfelder, Curtiss, Bird, & Mayer, 1964). The first approximation $[D]_1$ at zero field for particles much larger and heavier than the gas molecules is directly related to electrical mobility through the Einstein's relation ($zeD = Z_p kT$) which then reveals from eq. (4):

$$[D]_1 = \frac{3}{16(n+N)}\left(\frac{2\pi kT_{eff}}{m_{red}}\right)^{1/2}\frac{1}{\bar{\Omega}_{1,1}(T_{eff})} \tag{32}$$

where in general ($n \gg N$). The correction term Δ is composed of a series of complicated approximations. The first approximation may be given by $\Delta \sim \zeta \left(\frac{N}{n+N}\right) \alpha_T/5$ and where ζ is a dimensionless constant dependent on the nature of the gas molecule's scattering and α_T is the thermal diffusion factor, a parameter that relates the diffusion coefficient to the thermal diffusion coefficient (Annis, Malinauskas, & Yun, 1970; E. Mason, Malinauskas, & Evans Iii, 1967; Monchick et al., 1963). With all accounted for, an expression for the mobility can be written as:

$$Z_p = \frac{1+\zeta_1\left(\frac{2\lambda}{d_p}\right)\left[\frac{1+\zeta_2\left(\frac{2\lambda}{d_p}\right)}{1+\zeta_3\left(\frac{2\lambda}{d_p}\right)}\right]}{3\pi\eta d_p} \tag{33}$$

And where the ζ_i variables are given by:

$$\zeta_1 = \frac{9PA}{4\bar{\Omega}_{1,1}} \quad ; \zeta_2 = \left(N\alpha_Q d_p m\bar{c}\right)(\mu\alpha_L) \quad ; \zeta_3 = \left(1 - \frac{1}{5}\zeta\alpha_L\right)\zeta_2 \tag{34a-c}$$

Here $\bar{c} = (8kT/\pi m)^{1/2}$ is the average gas thermal velocity and α_Q and α_L are the Lorentzian and quasi-Lorentzian values of the thermal diffusion factor related to the thermal diffusion factor by: $(N+n)/\alpha_T = N/\alpha_L + n/\alpha_Q$(E. Mason et al., 1967). These values are also dependent on the nature of the scattering and therefore their value is difficult to assess except for particular cases, e.g. specular collisions. In all, the ζ_i parameters should be treated like adjustable constants. When compared to the A_i parameters from Stokes-Millikan, a correlation can be made:

$$\zeta_1 = A_1 \; ; \; \zeta_2 = \frac{A_1 + A_2}{A_1 A_3} \quad ; \quad \zeta_3 = 1/A_3$$

While Annis's result does not seem to improve upon the result of Millikan, it presents an additional description of the parameters that did not previously exist and gives further validity to the model.

Within the free molecular regime, further improvements may be implemented to increase the accuracy of the Stokes-Millikan equation. To account for potential interactions, Mason and Chapman initially proposed an enhancement factor $\bar{\Omega}_{1,1} = \xi PA(1 + S/T)$ where S is the Sutherland constant (Edward A Mason & Chapman, 1962). This concern was later picked up by Tammet (Tammet, 1995), who, taking into account the results from Epstein and Millikan, offered a correction for the collision cross section similar to eq. (7), but with an enhancement factor. Given that the longest range interaction is that of the ion-induced dipole potential, with $U_{pol} = -2\alpha_p(ze)^2/\pi\epsilon_0\left(d_p + d_g\right)^4$ with α_p being the polarizability of the gas, Tammet proposes a $\infty - 4$ potential correction for eq. (7) as:

$$\bar{\Omega}_{1,1}(T) = (\xi + \bar{\Omega}^*{}_{\infty-4} - 1)PA \tag{35}$$

Here PA is now assumed to contain the non-negligible addition of the gas diameter d_g for small particles, and where $\bar{\Omega}^*{}_{\infty-4}$ is as a function of the dimensionless potential $\varphi_e = \frac{U}{kT}$:

$$\bar{\Omega}_{\infty-4} = \begin{cases} 1.4691(\varphi_e)^{1/2} - 0.341(\varphi_e)^{\frac{1}{4}} + 0.185(\varphi_e)^{\frac{5}{4}} + 0.059 \; ; \quad if \; \varphi_e \geq 1 \\ 0.106(\varphi_e)^1 + 0.263(\varphi_e)^{\frac{4}{3}} + 1 \; ; \quad if \; \varphi_e \leq 1 \end{cases} \tag{36}$$

with

$$U = \begin{cases} \infty \quad if\ position\ r < d_p + d_g \\ U_{pol}\ if\ position\ r > d_p + d_g \end{cases}$$

To get eq. (36), Tammet used the tables provided by McDaniel and Mason(McDaniel & Mason, 1973). Considering the reduced mass, Tammet proposed a modified Stokes-Tammet-Millikan equation:

$$Z_p = f_1 f_2 \frac{ze}{3\pi\eta(d_p+d_g)}\left\{1 + \frac{2\lambda}{d_p+d_g}\left(A_1 + A_2\, exp\left[-\frac{A_3(d_p+d_g)}{\lambda}\right]\right)\right\} \quad (37)$$

Here $f_1 = \left(1 + \frac{m_{gas}}{m_w}\right)^{1/2}$ and the second factor relates to the effects of scattering and potential interactions:

$$f_2 = \frac{9/4}{(A_1+A_2)\left(\xi(d_p+d_g,T)+\bar{\Omega}_{\infty-4}(T)-1\right)} \quad (38)$$

Tammet used empirical data from Kilpatrick to get an expression for ξ proving the validity of eq. (37) for a range of masses from 35.5-2122 Da(Kilpatrick, 1971). Tammet also assumed a correction from mass diameter to mobility diameter through an additional increment he labeled “extra distance”.

Larriba-Andaluz and Hogan proposed a similar correction to that of Tammet regarding the interaction potential(Larriba & Hogan, 2013b). They did so through their own numerical calculations, focusing only on the free molecular regime. They suggested a potential correction $\mathcal{L}$ that takes into account the ion-induced ion potential providing the approximation:

$$\bar{\Omega}_{1,1}(T) = \mathcal{L}\xi PA \quad (39)$$

Where $\mathcal{L}$ is given by:

$$\mathcal{L} = \begin{cases} 1 + \varphi_e\left(\frac{1}{3.1} + \frac{1}{\xi}\left(\frac{1}{16} + \frac{4}{33}\varphi_e\right)\right) \;\; ; \;\; if\ \varphi_e \le 1 \\ 1 + \varphi_e\left(\frac{1}{4} - \frac{2.3}{1000}\varphi_e + \frac{1}{\xi}\left(\frac{9}{56} - \frac{6.8}{1000}\varphi_e\right)\right) \;\; ; \;\; if\ \varphi_e \ge 1 \end{cases}$$

When compared to eq. (28), $\mathcal{L}$ also includes the coupling of scattering effects and potential interactions as well as the effect of grazing gas molecules, i.e., gas molecules that do not directly impinge on the charged particle but are still deflected and cause a momentum transfer. The results of eq. (39) have been shown to be in agreement with experiments for a series of tetralkylammonium salts and other non-spherical ions.

3. Electrical Mobility of particles with arbitrary shape: Analytical and Computational approaches.

3.1. Calculations of non-spherical entities in the Transition regime.

Prior to treating the electrical mobility of an arbitrary particle within the transition regime, it is perhaps beneficial to briefly describe the process in the continuum regime. In principle, the mobility of a particle of arbitrary shape can be calculated in the continuum regime by solving the Stokes (i.e., creeping flow) equations for the flow field around the particle and use the solution to integrate the calculated viscous and pressure forces over the wetted surface to obtain the value of the drag force (Filippov, 2000; Landau & Lifshitz, 1975). The latter naturally leads to the definition, via the Stokes Law in Eq. (1), of a hydrodynamic diameter (d_H) which is the diameter of a perfect sphere that would experience the same hydrodynamic drag force of the particle under investigation. In theory and with sufficient computational resources to solve the Stokes equation, the approach could be extended to the near-continuum portion of the transition regime, if

one can pre-determine appropriate slip boundary condition at the particle wetted surface. In reality, the applicability of the Stokes continuum approach is limited not only by the complexity of determining the (spatial distribution of the) slip boundary conditions but also to the existence of multiple length scales when dealing with particles of arbitrary geometry (e.g., fractals). Indeed the Stokes equation of motion of a continuum fluid may not be an acceptable model in some bay zones of the particle whose size is comparable to the mean free path of the gas, even when the overall size of the particle is much larger and well within the continuum regime.

Progressing into arbitrary particles well within the transition regime, one can no longer fully rely directly on the Stokes-Millikan equation, despite its extensive success, as its validity is, at least in principle, limited to spherical particles. However, it is quite possible that, with proper corrections, one could arrive at variations of the equation that may yield acceptable results. To understand the corrections involved, it is necessary to first define at least one characteristic size for the arbitrary charged particle (DeCarlo, Slowik, Worsnop, Davidovits, & Jimenez, 2004). While many different definitions exist of such parameters, we shall limit ourselves here to four different definitions, the physical diameter (d_c), the volume equivalent diameter (d_{ve}), the mobility diameter (d_p) and the hydrodynamic diameter (d_H). The physical diameter, d_c, is the simplest characterization of a geometric parameter. Unless the particle is spherical, d_c does not have a precise definition. It may be defined as the diameter of a sphere that would yield the same size measurement as the particle under consideration. This physical diameter will therefore depend on the type of measurement. The volume-equivalent diameter, d_{ve}, is the diameter of a sphere that has the same volume as the particle in consideration. This volume is quite useful in the sense that the resulting volume of the sphere relates mass and density through the well-known relation $\rho = m_w/V_p$. The mobility diameter, d_p, is defined as the diameter of a sphere with the same drift velocity as the charged particle migrating through a buffer gas by means of an electric field. If employed in the continuum, e.g. eq. (3), d_p agrees with the hydrodynamic diameter d_H, which establishes a physical descriptor of the object independent of the fluid properties (Chen, Weakliem, & Meakin, 1988; Hubbard & Douglas, 1993). However, if d_p is employed in the free molecular regime, it is better associated to the closest physical descriptor of the CCS, which would be the orientationally averaged Projected Area (PA).

While the definition of d_p may seem precise, this is far from being the case. The reason is that the value of d_p depends on the type of Stokes-Millikan approximation used to obtain it, and the set of conditions considered e.g., pressure, temperature, electric fields, regime, etc... When dealing with non-spherical particles, instead of using d_p to loosely describe a particle with a particular electrical mobility, it is reasonable that both d_{ve} and d_H could be used as a physical descriptor parameter within the Stokes-Millikan equation. With the inclusion of these physical descriptors, an additional correction is necessarily required, something that Tammet referred to as the "extra distance". To do so, a correction labeled the dynamic shape factor χ_m initially discussed by Fuchs was introduced into the Stokes-Millikan equation, (N. A. Fuchs et al., 1965). The approach was subsequently explored by Dahneke through what he termed adjusted sphere approximations (B. E. Dahneke, 1973a, 1973b, 1973c). The dynamic factor may be defined as the ratio of the drag force of the non-spherical particle to the drag on the volume-equivalent sphere (Hinds, 1999):

$$\chi_m(Kn) = \frac{F_D}{F_{D\,ve}} \tag{40}$$

The Stokes-Fuchs-Dahneke-Millikan equation thus becomes:

$$Z_p = \frac{ze}{3\pi\eta(d_{ve})\chi_m(Kn)}\left\{1 + \frac{2\lambda}{d_{ve}}\left(A_1 + A_2\, exp\left[-\frac{A_3 d_{ve}}{\lambda}\right]\right)\right\} \tag{41}$$

There are some interesting repercussions to this equation. If the dynamic shape factor χ_m and electrical mobility are known, the resulting diameter calculated from eq. (41) could be directly related to its mass and density. The difficulty in eq. (41) comes from identifying adequate relations for χ_m, as the dynamic factor changes not only with particle shape and flow regime (CHENG, 1991), but also with orientation (B. E. Dahneke, 1973a; Hinds, 1999). The orientation phenomenon itself is something very difficult to characterize as it is generally accepted that streamlined nonsymmetrical shapes or charged particles with strong dipole moments may orient themselves in the flow. Nonetheless, even in these simplest cases, the particle orientation would fluctuate around the preferred spontaneous direction because of its unavoidable Brownian/thermal rotational diffusion.

A few numerical approaches have been proposed for modeling the mobility of non-spherical aggregates across the entire Knudsen range. Given that two limiting physical descriptors in the continuum and free molecular regimes are the hydrodynamic diameter and the PA of the particle, respectively, one can try to provide a universal law for all aggregates by making use of a modified Knudsen number in the Stokes-Millikan equation (Zhang, Thajudeen, Larriba, Schwartzentruber, & Hogan Jr, 2012):

$$Z_p = ze\frac{1+Kn_{mod}\left(A_1+A_2 exp\left(-\frac{2A_3}{Kn_{mod}}\right)\right)}{3\pi\eta d_H} \quad ; \quad Kn_{mod} = \frac{2\lambda}{d_H}\frac{\pi d_H^2}{4PA} = \frac{\lambda\pi d_H}{2PA} \tag{42}$$

The purpose of the modified Knudsen number is clear. It is meant to provide asymptotically correct descriptions of any aggregate throughout any flow condition using a single equation. If $Kn_{mod}\sim 0$, then the electrical mobility is given by Stokes law using the hydrodynamic diameter. If on the contrary $Kn_{mod} \gg 1$, one arrives at the free molecular expression in eq. (4). This will happen as long as the condition $\Omega_{1,1}\sim 1.36PA$ holds true in the free molecular region, something further addressed in the next section. Based on the assumption that the modified Knudsen number $\lambda\pi d_H/2PA$ must asymptotically match both the continuum and the free molecular regime, perhaps one can propose an improvement of the Stokes Millikan equation that more closely follows the expected results of the free molecular regime, for example considering a CCS of the type $\Omega_{1,1}\sim\mathcal{L}\xi PA$. This correction would suggest a secondary expression for the Knudsen number $Kn_{corr} = \lambda d_H/2\Omega_{1,1}$ that may be employed for a more universal characterization.

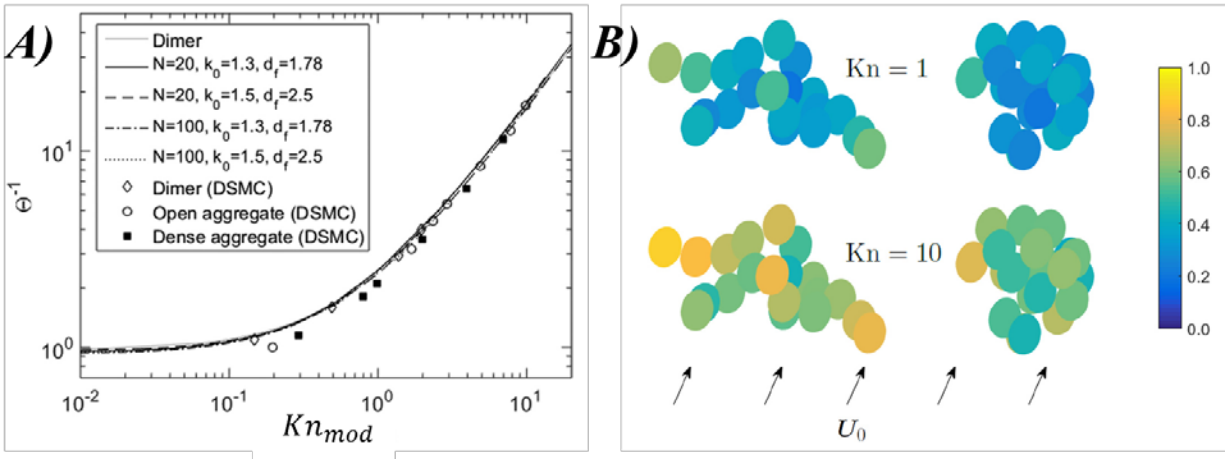

Figure 4. A) Calculated slip correction factors for different aggregates as a function of the modified Knudsen number (eq. (42)) and where $\Theta^{-1} = Z/Z_{continuum}$. Symbols refer to the DSMC results from Zhang et al(Zhang et al., 2012). Lines are results from Corson et al. (Corson, Mulholland, & Zachariah, 2017). B) Shown as a color scheme is the ratio of drag force on an aggregate sphere to the drag force on the same sphere isolated from the aggregate. Open and closed aggregates are shown for two different Knudsen numbers. Both figures have been adapted from Ref. (Corson et al., 2017).

For this reason, the use of Kn_{mod} together with Stokes-Millikan in eq. (42) should work to numerically describe any aggregate's mobility that is assumed to have a predominantly diffuse reflection of the gas molecules. In fact, the calculation of d_H and PA would result in the same accuracy as the more theoretically convoluted methods described below.

A valid approach to describe the electrical mobility and other transport related quantities of non-spherically shaped particles is through the use of Direct Simulation Monte Carlo (DSMC) simulations (Zhang et al., 2012). Zhang et al. show that the numerical calculation of the drag through DSMC leads to a close agreement with eq. (42) (Zhang et al., 2012), as shown in Figure 4A. Given that DSMC is meant to be used in rarified gases, the calculation becomes rather computationally expensive for small Knudsen numbers and might underpredict the results due to statistical errors as the continuum regime is approached. However, the simulations are quite accurate for larger Knudsen numbers typical of transition and free molecular regime. The fact that different non-spherical particles can be grouped into a single equation, suggests the broad applicability of a correction factor, at least to a degree.

Aside from DSMC simulations, there are a number of theories regarding the calculation for aggregates within the transition regime (Melas, Isella, Konstandopoulos, & Drossinos, 2014, 2015; Sorensen, 2011). Perhaps, most prominent are those making use of the Kirkwood-Riseman (KR) theory to calculate the drag on fractal aggregates composed of spherical elements. While the KR theory was initially meant to be used within the continuum regime (Kirkwood & Riseman, 1948), it has been recently extended to be used in the transition regime (Corson et al., 2017). The idea behind the KR theory consists in calculating the drag on individual spherical chain elements and then adding them together. However, the drag on each element should necessarily depend on the surrounding elements in such a manner that the interior elements may partially be hydrodynamically shielded from the outside flow and hence contribute less to the overall drag. This shielding effect will depend on the Knudsen number and distance between spheres, with the shielding efficiency decreasing with both higher Kn and relative distance. In general, the drag on the lth element of an aggregate that is held in place in a gas flowing with uniform velocity U_{∞_i} maybe given by:

$$F_{D_{l_i}} = f_f v_{d_i} = f_f (v_{l_i} - u_{l_i}) \tag{43}$$

In the above equation, v_{l_i} represents the velocity that the fluid would possess at the location of the lth sphere in the absence of the sphere and u_{l_i} represents the velocity of the lth element with respect to the fixed position, i.e. the relative velocity due to the rotation or flexible deformation of the aggregate. Assuming that the velocity of rotation is negligibly small and that the aggregate is rigid, an approximation that is regularly done in aerosols is to consider u_{l_i} to be 0, at least on average. The fluid velocity v_{l_i} may be calculated as the sum of the unperturbed velocity U_{∞_i} in the absence of the aggregate minus the sum of the shielding perturbations v'_{lk} created by the rest of the kth elements of the aggregate. To provide an expression for v'_{lk}, one can use the Oseen tensor formula, which provides the velocity perturbation on the surface of the lth element caused by the presence of the kth element drag force, F_{D_K} (Burgers, 1938). In all, the $F_{D_{l_i}}$ may be rewritten as:

$$F_{D_{l_i}} = f_f v_{l_i} = f_f U_{\infty_{l_i}} - \sum_{l \neq k}^{n} f_f v'_{lk_i} \;\; ; \;\; v'_{lk_i} = T_{lk_{ji}} \cdot F_{D_{k_j}} \tag{43'}$$

$$T_{lk} = \frac{1}{8\pi\eta r}\left\{\left[\bar{\bar{I}} + \frac{\overline{\overline{r_{lk} r_{lk}}}}{r}\right] + \left(\frac{2a^2}{r^2}\right)\left[\frac{1}{3}\bar{\bar{I}} - \frac{\overline{\overline{r_{lk} r_{lk}}}}{r^2}\right]\right\}, \tag{44}$$

where T_{lk} is the modified Oseen tensor, a is the radius of the spheres composing the aggregates, r_{lk} is the vector distance between the centers of the lth element to the kth element, and r is the magnitude of said distance. The original Oseen tensor was different from eq. (44), and was equivalent to assuming a single

point force ($a \to 0$) in eq. (44). However, as noted by Rotne and Prager and Yamakawa, it was not positive definite (Rotne & Prager, 1969; Yamakawa, 1970). When the force is distributed uniformly on a spherical surface of radius a, the solution for the hydrodynamic interaction tensor requires a Taylor series around $a \to 0$. If only a first order correction is taken into account, the hydrodynamic tensor is very similar to that of eq. (44) but the second term is missing a factor of 2. The factor of 2 appears in the first order correction term when the interaction is considered to be between two spheres of radius a, instead of a single sphere. Other authors have studied higher order corrections and multi-body interaction tensors as well (Carrasco & Garcıa de la Torre, 1999; Goldstein, 1985; Mazur & van Saarloos, 1982; Reuland, Felderhof, & Jones, 1978).

Due to the convoluted nature of the shielding effects, the drag forces on each individual sphere must all be calculated simultaneously by solving a linear system of equations (43). The total drag force on the aggregate is then inferred by summing of all the forces from individual spheres. Chen, Deutch and Meakin used these results to obtain the overall translational friction coefficient of the aggregate (Chen, Deutch, & Meakin, 1984; Meakin, Chen, & Deutch, 1985) and where the individual friction factor f_f was assumed equal to the $6\pi\eta a$ value expected in the continuous regime. However, the same approach may perhaps be expanded to include the transition and free molecular regime conditions by using the friction factor f_f represented by the Stokes-Millikan equation of a single sphere, and hence mobility and/or diffusion may then be calculated for the entire Knudsen range using an extended KR theory. However, the modified Oseen tensor, which was inferred for the continuum regime, does not provide a correct interpretation of the perturbations within the transition and free molecular regimes and a corrected perturbation tensor must be employed.

Instead of using the Stokes-Millikan equation to obtain f_f, another option is to obtain the friction factor f_f by solving the BGK equation that describes a perturbed gas flow over a sphere. A numerical value of f_f for a sphere using the BGK approach was obtained by Loyalka et al. and by Takata et al. following the results of Cercignani (Law & Loyalka, 1986; Lea & Loyalka, 1982; Takata, Sone, & Aoki, 1993). The difference between the results for the friction factors of the two approaches is around 2-3% which validates the BGK approach (Corson et al., 2017). Interestingly enough, the BGK approach allows one to describe the perturbation over a sphere as a function of the Knudsen number. This perturbation may then be used as a substitute of v'_{lk_i} and replacing the Oseen Tensor and force in eq. (43). This perturbation is only for the presence of a single sphere and not for a sphere-sphere hydrodynamic interaction but the similarity shown in the continuum between the two effects is sufficient to consider this approach. Corson et al. used the results from Loyalka and Takata together with the KR theory to obtain the drag on aggregates for any Knudsen number (Corson et al., 2017). The results from Corson et al. are compared to those of Zhang et al. in Figure 4A for different aggregates to support the validity of both approaches, so that the use of the modified perturbation seems to be an acceptable approximation. To visualize the effect that the perturbation of the aggregate has on individual spheres, Corson et al. provides a ratio of the drag from eq. (43) to the drag corresponding to each isolated sphere (first term of eq. 43) as shown in Figure 4B. One can easily observe how the flow interaction between the different individual spheres becomes progressively less important as one gets closer to the free molecular regime.

It is interesting to note here that the work from Corson et al.'s work makes use of eq. (25), instead of eq. (26), to provide an orientationally averaged value for the mobility assuming that all orientations are considered to be equally probable. However, in the presence of strong fields within the transition regime, the assumption that all orientations are equally probable is most likely no longer be satisfied. Corson et al. expanded on their work to calculate the mobility of a perfectly conducting particle by adding a polarizability tensor to the calculation which would affect particle orientation (Corson, Mulholland, & Zachariah, 2018).

3.2. Use of the slip correction to calculate collision kernels for particles of arbitrary shape.

An interesting use of the Stokes-Millikan approach that is worth mentioning here due to its success and broad applicability, is its use in the calculation of collision kernels between particles in the transition regime. The existing calculations, however, are mostly based on understanding coagulation between two aerosol particles rather than electrical mobility(Rogak & Flagan, 1992). In the transition and continuum regimes, the collision frequency, β_{ij}, is defined using diffusion coefficients D_i rather than electrical mobility:

$$\beta_{ij} = 4\pi\left(D_i + D_j\right)\langle d_{ij}\rangle\chi_k(Kn) \quad ; \quad D_i = kTZ_{pi}/ze \tag{45a-b}$$

Where $\langle d_{ij}\rangle$ is an equivalent average diameter of the two colliding entities and $\chi_k(Kn)$ is a correction factor, similar to the dynamic factor, that is a function of the Knudsen number or a seemingly related dimensionless quantity (Diffusion Knudsen or momentum transfer Kudsen number). The exact values of the correction factor $\chi_k(Kn)$ are a subject of debate and multiple equivalent formulas have been used. The factor was initially calculated by Fuchs through the flux-matching model (N. Fuchs, 1963; N. A. Fuchs et al., 1965). A simpler approximation was provided later on by Dahneke (B. Dahneke, 1983). Other modifications have surfaced (Fuks & Sutugin, 1970; Veshchunov, 2010a, 2010b), including approximations in the free molecular regime, some of them quite complex but very successful even for non-spherical entities (M Zurita-Gotor & Rosner, 2002). Gopalakrishnan and Thajudeen et al. provide the most recent additions for collision kernels for the complete Knudsen range making use of the Langevin equation (Gopalakrishnan & Hogan Jr, 2011; Gopalakrishnan, Thajudeen, & Hogan Jr, 2011).

3.3. Calculations of non-spherical ions and charged nanoclusters in the Free-Molecular Regime.

3.3.1. Background and discrepancies between aerosol and analytical chemistry fields

Due to the set of simplifications that arise in the free molecular regime, and the realization that the momentum transfer of each individual gas molecule collision is independent of the rest, the calculation of electrical mobility for non-spherical ions is much more feasible than in the transition regime. As such, there are plenty of different approximations to the calculation of mobilities using gas kinetic theory. As previously introduced, two methodologies stand out which arise from the study of ion/electrical mobility from the point of view of two different scientific fields, analytical chemistry, and aerosol science. While the results from the two approaches may seem to differ at first, it turns out that many of the results from both fields are equivalent to each other, the largest disparities being related to the distinct concerns of the two fields. It is sufficient to say at this point that while analytical chemistry focuses on small ions with strong potential interactions and for which the diffuse accommodation assumption has been shown to break down (especially in light gases such as He), aerosol science focuses on relatively larger singly charged nanoclusters, fractals, and particles, for which the effect of interaction potentials and reduced masses are mostly negligible. Additionally, the diffuse reflection assumption is unequivocally and somewhat arbitrarily chosen so as to match the Millikan results in the transition regime. As a result, the perceived differences between the two fields mostly originates from how the different approaches tackle the transition from specular to diffuse collisions, although there is little doubt that the transition exists (C. Larriba-Andaluz, Fernandez-Garcia, Ewing, Hogan, & Clemmer, 2015; Z. Li & Wang, 2003a, 2005). How this transition occurs is a subject of debate although a majority agrees that the modality depends on the buffer gas, the conditions of the electric field, the size of the ions, as well as the mass of the individual atoms compared to the mass of the gas molecule.

In either case, the necessity of aerosol science to study nucleation, coagulation and surface growth in detail requires the characterization of particles of ever-decreasing sizes, together with the necessity for analytical chemistry to provide more accurate and efficient calculations for macro-ions and large biomolecules, has led to a greater interaction between the two fields and the procurement of common ground. A detailed study of the approach from the analytical chemistry perspective is out of the scope of this review but a brief summary is provided here for the sake of completeness although the reader is prompted to consult the relevant literature, if required.

3.3.2. Free Molecular Mobility/Drag analytical and numerical calculations for non-spherical particles.

Equation (23) is one of the most general expressions that may be used when dealing with the calculation of drag in the free molecular regime. Since no potential interactions are used to obtain eq. (23), as long as the wetted area of the charged particle is known, the equation can be solved analytically for a given accommodation coefficient, but not without certain complications. Following the Epstein's approach, Dahneke produced an analytical study of different convex particles including discs, cylinders, prolate and oblate spheroids and cubes (B. E. Dahneke, 1973b). Garcia-Ybarra and Rosner studied sphero-cylindrical particles (cylinders with spherical caps at the end)(Garcia-Ybarra & Rosner, 1989), de la Mora made a comprehensive study of different convex polyhedra with a focus on how the existence of principal axis of the molecule facilitates the calculation process (Fernández de la Mora, 2002), and Larriba and de la Mora provided analytical calculations for beads on a string configurations to study polymer structures in the gas phase (Larriba & Fernandez de la Mora, 2012). Except perhaps for the bead on string polymeric studies, all the structures studied analytically are convex. The reason for the prevalence of convex structures is that concave surface elements may prevent some of the surface area from being accessible to gas molecules while also leading to the possibility of multiple scattering. Both effects are significantly difficult to assess analytically but need to be considered in the calculation of the overall drag force. Perhaps the only available analytical solution of a free molecular transport property for particles which can be locally concave has been given by Zurita-Gotor (Mauricio Zurita-Gotor, 2006). Chan and Dahneke, on the basis of some results by Chahine (Chahine, 1961), observed that the analytical calculation of such effects on concave structures is futile in a practical way (Chan & Dahneke, 1981) and proposed the use of a Monte Carlo technique, previously described by Bird (Bird, 1976), to deterministically predict the scattering within the concave regions. This Monte Carlo approach led to a lot more flexibility on the types of structures that could be calculated and was later picked up by Zurita-Gotor and Mackowski who applied it to fractals to calculate thermophoretic and electrohydrodynamic drag forces (Mackowski, 2006; Zurita, 2004). In the Monte Carlo approach, the particle is fixed inside of a cuboid domain assumed to have a constant drift velocity. The particle is not flexible and is not allowed to rotate. From the assumed velocity distributions (eqs. 8 and 10), fluxes of gas molecules entering the domain through the walls of the cuboid are calculated analytically using higher order moments. With the provided fluxes, hundreds of thousands of gas molecules are then statistically inserted in the domain and allowed to traverse and interact with the particle until they leave the domain. The drag force is therefore calculated as the total momentum transfer (final minus initial) per unit time of the sum of all the gas molecules studied:

$$\vec{F}_D = \frac{\sum_{i=1}^{i=N_t} m_w(\vec{g}_f - \vec{g}_i)}{\tau_t}. \tag{46}$$

Here N_t is the total number of gas molecules and τ_t is the total time that it takes for all N_t molecules to enter the domain. This method of drag calculation has been known in other fields as the momentum-transfer theory for how the momentum balance plays an important role in the calculation (Edward A. Mason & McDaniel, 1988). The calculation is repeated for three perpendicular directions so that a drag tensor maybe

provided akin to that of eq. (24) and appropriately averaged to obtain the mobility. Mackowski used the algorithm to calculate only diffuse or specular interactions for fractals. However, this Monte Carlo approach allows for potential interactions to be added as well, which will become necessary when studying molecular and entities with resolved atomic structure. A cartoon of the Monte Carlo domain approach is provided in Figure 5A.

At this stage of the discussion, one may be able to appreciate some of the calculations that were performed in the field of analytical chemistry which consider, almost exclusively, entities with resolved atomic structure that are strictly within the free molecular regime. While, in principle, the quadrature in eq. (9) may be calculated analytically for very basic structures and potentials, the calculation of the deflection angle χ_{def} for complex structures is too cumbersome to be carried out efficiently. For this reason, eq. (9) is almost exclusively calculated numerically using Monte Carlo simulations. As seen previously, a very simple calculation that replaces eq. (9) consists in assuming an averaged Projection Approximation (PA) for the ion (Von Helden, Hsu, Kemper, & Bowers, 1991). This would exclude any scattering or potential interaction as depicted in blue in figure 5B. The calculation of the PA is equivalent to projecting the shadow of the particle in multiple random directions and averaging the total result. When compared to eq. (23), PA would yield equivalent results if $\alpha = 0$ and the particle was convex. If the particle were not convex, the results from PA would be equivalent to calculating eq. (23) using the convex hull as the surface area and $\alpha = 0$.

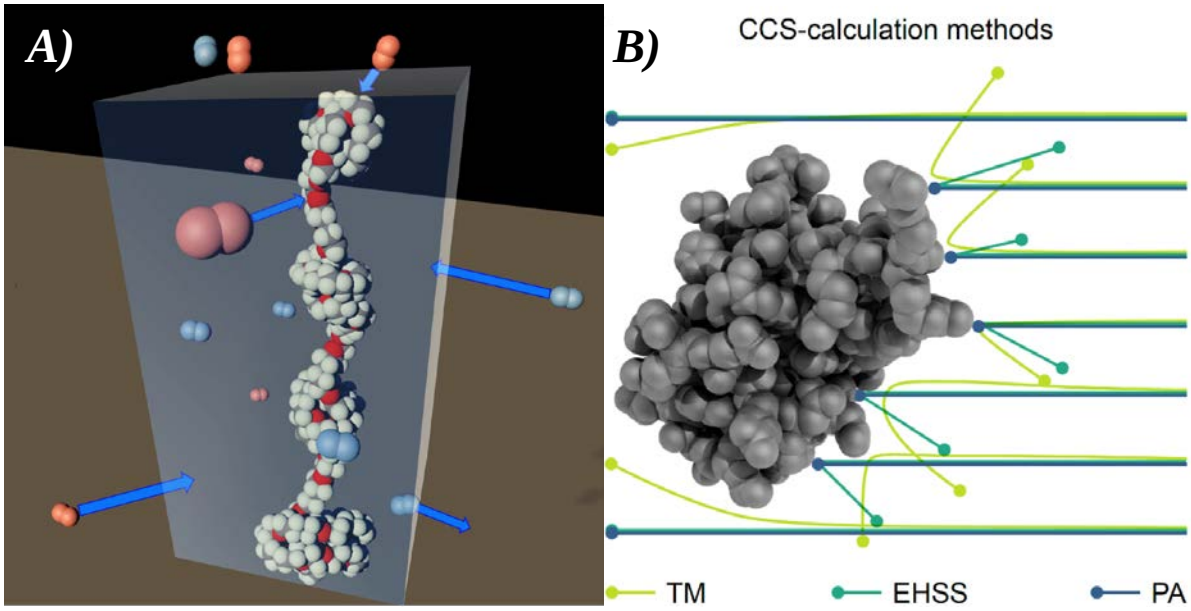

Figure 5. A) Depiction of the Monte Carlo domain approach to deterministically calculate the drag force and electrical mobility of a particle in the free molecular regime by calculating the momentum transfer of gas molecules entering and exiting the cuboid. 5 B) Basic CCS calculation methods to solve eq. (9), which include the Trajectory Method (TM), the Exact Hard Sphere Scattering (EHSS), and the Projection Approximation (PA). TM Method considers a 4-6-12 interaction, EHSS considers elastic specular scattering, and PA only differentiates between collisions and fly-by unperturbed trajectories. Figure 5B has been extracted from Ref. (Gabelica & Marklund, 2018).

The first widely used calculator that took full advantage of eq. (9) was MOBCAL by Jarrold and co-workers (Shvartsburg & Jarrold, 1996). Aside from the PA method, two different calculations are possible in MOBCAL, the Exact Hard Sphere Scattering (EHSS) and the Trajectory Method (TM)(Mesleh, Hunter, Shvartsburg, Schatz, & Jarrold, 1996). In the EHSS method, the all-atom structure is fixed in space and oriented randomly, and gas molecules are sampled from randomly oriented plane assuming rectilinear trajectories perpendicular to the plane. Collisions with the structure are assumed to be specular and elastic

as depicted in Figure 5B in light green. Upon reflection, the gas molecules are allowed to collide with the structure again multiple times (referred to as multiple scattering). The multiple scattering has an enhancing effect of the momentum transfer that most of the time increases the value of the CCS compared to that of PA. After several gas molecules are sampled, the structure is re-oriented and the process is repeated. Once sufficient orientations are considered, an average drag is calculated assuming all orientations are equally probable. Given that eq. (9) comes from a quadrature where a condition of elasticity has been utilized, diffuse/inelastic collisions are slightly harder to implement and hence no diffusive version may be performed within MOBCAL. EHSS has been shown to provide accurate CCS calculations for Helium gas for a wide range of particle sizes but fails to produce reasonable predictions for heavier and diatomic gases, including Argon, Nitrogen, and Air, which seem to require more inelastic and diffuse collisions. This suggests that the global modality of reflection of gas molecules is different depending on the gas. Additionally, given that an accommodation coefficient of ~0.91 has been used successfully for large charged particles even in He (Eglin, 1923; Ishida, 1923; Rader, 1990), it appears that, even within the same gas, there must be an evolution from specular to "effectively" diffuse collision as the Knudsen number is decreased.

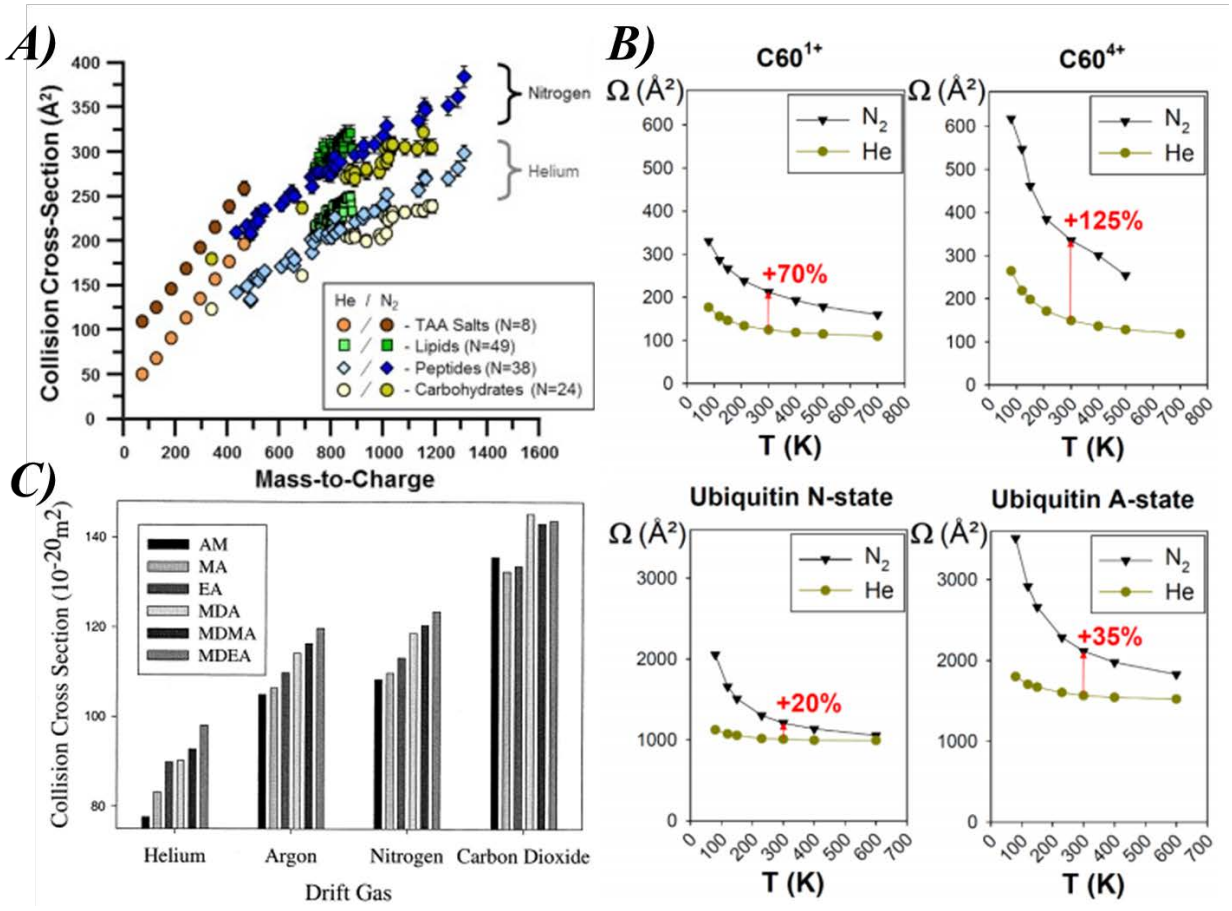

Figure 6. Comparison of different CCS from different gases. Figures were directly taken from Refs. (Gabelica & Marklund, 2018; Leaptrot, May, Dodds, & McLean, 2019; Matz, Hill, Beegle, & Kanik, 2002). A) CCS in Helium and Nitrogen for different sets of ions. B) CCS for C60 and Ubiquitin Native and Open (see legend) states in Nitrogen and Helium at different temperatures. C) CCS of several amphetamines under Helium, Argon, Nitrogen and Carbon Dioxide environments (see legend).

In the TM method, gas molecules are subject to interaction potentials with the different elements composing the ion or particle. The interaction potentials Φ were initially limited to the induced-dipole potential and Lennard-Jones (L-J) potentials(Mesleh et al., 1996):

$$\Phi(x,y,z) = 4\epsilon \sum_{i=1}^{n_t} \left[\left(\frac{\sigma}{r_i}\right)^{12} - \left(\frac{\sigma}{r_i}\right)^{6} \right] - \frac{\alpha_p}{2} \left(\frac{q_i}{n_z}\right)^2 \left[\left(\sum_{i=1}^{n_z} \frac{x_i}{r_i^3}\right)^2 + \left(\sum_{i=1}^{n_z} \frac{y_i}{r_i^3}\right)^2 + \left(\sum_{i=1}^{n_z} \frac{z_i}{r_i^3}\right)^2 \right] \quad (47)$$

Here, $r_i = (x_i, y_i, z_i)$ is the relative distance between the gas molecule and the ith atom/subunit/charge, α_p is the polarization constant of the gas, q_i is the ith charge, n_t is the total number of atoms/subunits, n_z is the total number of charges, and σ and ϵ are the zero cross and well-depth parameters for the L-J potentials. Similar to the EHSS case, the potential interaction is always elastic being the deflection angle χ_{def} the sole quantity obtained from the Monte Carlo simulation. The implementation of the TM to calculate CCS from small to medium ions has been incredibly successful in gases such as He and N_2. However, its success relies on the correct determination of the parameters of the L-J potentials for every atom/subunit composing the ion or particle. When these parameters are correctly optimized, the CCS results are regularly within 4% of the experimentally measured ones(Campuzano et al., 2012).

Given the diatomic nature of N_2, the effect of the quadrupole potential has been considered as an additional potential in eq. (47) (Kim et al., 2008). In it, the diatomic nitrogen molecule charge is divided into three charges, with a negative charge of 0.4825e on each nitrogen and a positive charge at the center of the molecule of 0.965e while assuming an interatomic distance of 1.0975 Angstroms. The quadrupole interaction potential, when reducing the quadrupole tensor to one term due to the linearity of the charges, is given by:

$$\Phi_{IQ}(x,y,z) = \sum_{j=1}^{3} \sum_{i=1}^{n_z} z_i z_j e^2 / r_{ij}^3 \quad (48)$$

Here r_{ij} denotes the distance from any i atom to the one of the 3 j charges in the N_2 molecule. Since the N_2 molecule is constantly rotating, the effect of the quadrupole is only important at very close range. An appropriately weighted parameter is used to take into account the relative orientation of the nitrogen molecule. A basic depiction of how the TM method interacts with an all-atom structure is represented using lime trajectories in Figure 5B (Gabelica & Marklund, 2018).

An interesting approach would be to adapt the domain approach of Chan and Dahneke and of Mackowski while considering interaction potentials. Larriba-Andaluz and Hogan followed Mackowski's approach and created a software suite labeled Ion Mobility Software (IMoS) with spherical as well as cuboid domains(Coots, Gandhi, Onakoya, Chen, & Andaluz, 2020; Larriba & Hogan, 2013a, 2013b), and where interaction potentials and entities with resolved atomic structure are considered. Aside from the EHSS, TM and PA calculations, IMoS is able to perform other multiple calculations, including rotational effects for diatomic gases (C. Larriba-Andaluz & Hogan, 2013). Since inelastic collisions may be introduced in the Monte Carlo domain approach, IMoS allows for a hybrid method that includes induced dipole potential and diffuse inelastic hard sphere scattering which is referred to as the Trajectory Diffuse Hard Sphere Scattering (TDHSS) method. When using this approach, the user can select the value of the accommodation coefficient α as well as the distribution of reemission velocities. The flexibility of this adjustment, when compared with other methods and experimental results, may shed light on how α varies within the free molecular regime and for different gases. The software was later parallelized and can perform calculations of particles composed of hundreds to thousands of atoms in seconds to minutes (Shrivastav, Nahin, Hogan, & Larriba-Andaluz, 2017a). When the same potential interactions are chosen with the same parameters, the results provided are within 1% of those of MOBCAL, but are obtained at a fraction of the computational cost.

To arrive at accuracies better than 4% for the prediction of CCS of entities with resolved atomic structure using the TM method, one must use well-defined model structures and optimized L-J parameters. The model structures should be obtained through ab-initio calculations or Density Functional Theory (DFT) (Hohenberg & Kohn, 1964). The DFT model structures, together with carefully obtained experimental CCS

values, can then be used to optimize the L-J parameters for every gas-atom pair (Campuzano et al., 2012; Wu, Derrick, Nahin, Chen, & Larriba-Andaluz, 2018). The tuned L-J parameters may then be used generally for similar substances. Once reliable numerical calculations are widespread and most CCS can be inferred within a few percent of the experimental counterpart, one has the possibility of testing the validity of the diffuse collision assumption of the Stokes-Millikan with relatively solid footing.

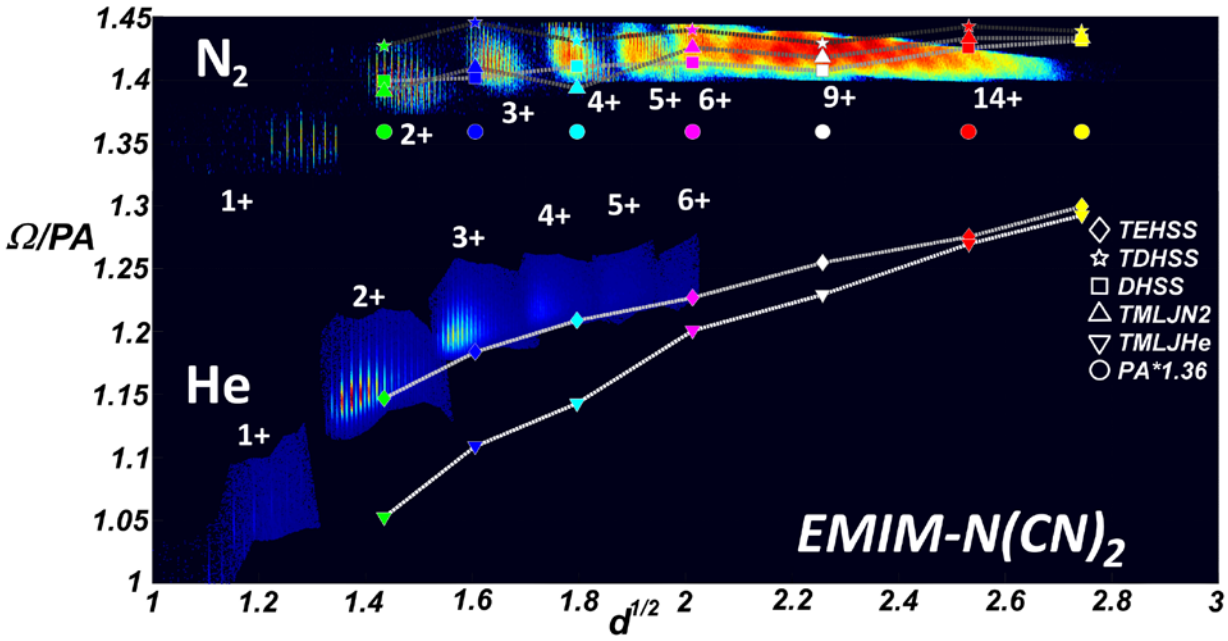

Figure 7. Dimensionless CCS as a function of the square root of the equivalent volume diameter for EMIM-N(CN)$_2$ under He and N2 environments. The symbols correspond to numerical calculations performed with IMoS using several collision models (see legend). Taken from Ref. (C. Larriba-Andaluz et al., 2015).

Regarding the diffuse assumption, given the success of elastic approaches within the TM, the first question that arises pertains to how the accommodation coefficient α is related to the ion-induced dipole and L-J potential interactions. The fact that experimental results for macromolecules in N_2 agree with TDHSS using $\alpha = 0.91$ as well as with results of TMLJ (4-6-12 interaction) (Shrivastav, Nahin, Hogan, & Larriba-Andaluz, 2017b), suggests that the collective effect of the attractive portion of the interaction potential on a sufficiently large molecule, causes the reflection to be "effectively" diffuse. This may be caricaturized as shown in Figure 3D where atoms adjacent to the one colliding with the molecule affect the gas trajectories through potential interactions resulting in a quasi-random direction of emission and without the need of imposing an arbitrary diffuse direction as it is done through the use of α. If such is the case, as the ion becomes smaller, the effect becomes smaller and the reflection becomes naturally more specular. In this descriptive framework, it is also possible that different gases – and different atoms- behave in different ways given that the interaction potentials may be quite different from each other. The effects that different gases have on the CCS have been extensively characterized and Figure 6 shows a few results comparing CCS of different ions for different gases and different temperatures (Gabelica & Marklund, 2018; Leaptrot et al., 2019; Matz et al., 2002). While part of the deviations between different gases may be associated with distinct polarizabilities, this cannot be the only factor providing the difference, especially for large singly charged entities. For example, Figure 6A shows the CCS as a function of the mass to charge ratio of several different types of analytes in He and Nitrogen gases. While the polarizability effect should be quite important for small mass to charge values (~100 Thomsons), it should become almost negligible for larger values, expecting its value to be lower than 3% in N_2 compared to He for ~1000 Thomsons. A similar trend

is also noticeable in Figure 6B. On the top of the figure, C60 fullerene CCS with 1 and 4 elementary charges are compared between He and N_2 gases as a function of the temperature. While the discussion below only focuses on room temperature, similar arguments may be used for other temperatures. The contribution of the ion induced dipole potential for a singly charged C60 at room temperature is approximately 5-6% larger in N_2 compared to He as calculated by IMoS. This is in contrast with the large difference of 70% observed experimentally. In the unlikely event that the 70% difference could be fully attributed to the ion-induced dipole potential, the same dipole effect would require that the difference would be much larger than 125% when 4 charges are present. The effect may be noticed also in the bottom panels of Figure 6B, where the difference between the CCS in He and N_2 is still about 20% even for a macromolecule such as Ubiquitin in its compact state at room temperature. Interestingly enough, when comparing all the results in Figure 6B, the difference between CCS in He and N_2 seems to be quite smaller for larger macromolecules even when correcting for the effect of the ion-induced dipole potential. This could indicate that the percentage of collisions that result in diffuse scattering becomes more similar for both gases as the size of the particles increases. Finally, even though the ion-induced dipole potential is not the sole effect that differentiates gases, its effect cannot be neglected especially for small molecules. As an example, Figure 6C shows the difference in CCS for different amphetamines in He, Ar, N_2 and CO_2.

Perhaps the best way to analyze how the scattering effect evolves in different gases is to employ a family of analytes that can be studied for a large range of mobility sizes. Ionic liquids may be used for such a purpose with the advantage that they form relatively spherical ions which may carry multiple charges. Studies by Larriba-Andaluz, de la Mora, and Clemmer using different Ionic Liquids in He and Nitrogen environments investigated the diffuse scattering effect (C. Larriba-Andaluz et al., 2015). One relevant result has been reproduced in Figure 7 for 1-3 Ethyl-Methyl-Imidazolium dicyanamide (EMIM-N$(CN)_2$) ion. Figure 7 plots the dimensionless CCS $\Omega/PA = \mathcal{L}\xi$ for EMIM-N$(CN)_2$ as a function of the square root of the volume equivalent diameter in Helium and Nitrogen gases. In the plot, within the resolved colored data, each of the vertical lines corresponds to an ion of a known mass (a certain number of neutrals and charges). The purpose of the choice of the square root of the diameter was to try to increase the visual separation of the smaller ions without the need to resort to logarithmic plots. When looking at the portion of the data measured in N_2, one can see that the value of Ω/PA remains fairly constant from 2nm ($d^{1/2} = 1.44$) to 8nm and where $\mathcal{L}\xi \sim 1.42$. Given that the ion-induced dipole potential effect is around 5-10% for the size/charge ranges being measured, the results suggests that $\xi \sim 1.33 - 1.36$ which agrees with the expected diffuse reflection from Stokes-Millikan and $\alpha = 0.9 - 0.91$. On the other hand, the $\mathcal{L}\xi$ value seems to decrease for charge states 1 and 2 in Nitrogen. Given that one would expect the effect of the ion-induced dipole to become increasingly more important with the reduction of size, the results appear to give the impression that the collisions become more specular as the ion is reduced in size. This is also corroborated by the numerical calculations done with IMoS and where TDHSS and TM agree to within 2-4% for the cases studied.

The results in Helium presented in Figure 7 are quite different from those presented in Nitrogen. The first thing to notice is that $\xi \sim 1.36$ is not reached in the range of mass-equivalent diameter values accessed experimentally. Moreover, for singly charged entities and ions close to 1nm, the results seem to suggest $\mathcal{L}\xi \sim 1$ and hence specular calculations or equivalently $\alpha \sim 0$. The value of $\mathcal{L}\xi$ increases steadily with the diameter of the ion hinting at an asymptotic value far from the observed experimental values. When compared to the numerical calculations from IMoS, the experimental values seem to agree quite well with the regular EHSS with ion-induced dipole interaction (TEHSS). Given that the potential interaction is minimal, most of the increment must be due to the increasing occurrence of diffuse scattering, i.e. multiple collisions occur for the same gas molecule, most likely due to the increasing roughness of the surface of the molecule. The numerical calculations performed suggest that the fraction of collisions resulting in

diffuse scattering will continue to increase with increasing size past our experimental data to a value of 1.3. Solely because of the multiple scattering on the surface, one can predict that eventually, the interaction may be considered “effectively” diffuse, matching the prediction of Stokes-Millikan and the asymptotic results for cases in the transition regime. Other authors, such as Li and Wang, have explained the specular to diffuse collision behavior through gas molecule trapping on the particle surface as observed from Molecular Dynamics simulation (Z. Li & Wang, 2005).

The fact that TDHSS agrees with TM in N_2 and that TEHSS qualitatively agrees with TM in He, seems to suggest that diffuse scattering effects may be embedded into the L-J parameters without loss of generality. However, the diffuse scattering effects may come in part from inelastic collisions (exchange of translational and ro-vibrational energies), especially in the case of N_2 and CO_2 where the gas molecule is much heavier than most of the individual atoms of an organic molecule such as an Ionic Liquid. Upon impact of a heavy gas molecule, it is very likely that the ion may deform in the region close to the collision, reducing the chances of a specular collision. This raises the question of whether heavier atoms could lead to more specular collisions for the same gas. Ouyang et al. studied this effect on alkali metal iodine salt clusters using cations of increasing mass in N_2. The results clearly show that, for very heavy atoms such as those in Cs-I and Rb-I salts, the resulting collisions are more specular while for less heavy atoms such as Na-I, the collisions become more diffuse (H. Ouyang, Larriba-Andaluz, Oberreit, & Hogan, 2013). This suggests that further studies using Molecular Dynamics instead of the presently used fixed structures should be important to ascertain the effects of inelastic collisions correctly.

The success of MOBCAL and IMoS has resulted in numerous other mobility calculators, mostly focused on optimizing and parallelizing MOBCAL, such as Collidoscope, HPCCS and Mobcal-MPI (Ewing, Donor, Wilson, & Prell, 2017; Ieritano, Crouse, Campbell, & Hopkins, 2019; Zanotto, Heerdt, Souza, Araujo, & Skaf, 2018). Mobcal-MPI changes the L-J parameters to a Buckingham type-based repulsion in an attempt to improve the accuracy of the calculation. Other calculators stem from convex to concave shape factor ratios such as the Projection Superposition Approximation (PSA), where the shape factor ratio directly multiplies the PA to give a relatively good approximation to the CCS(Bleiholder, Wyttenbach, & Bowers, 2011). Interestingly, this shape factor for large macromolecules varies around 1.3-1.39 on average, which suggests that, regardless of the gas or particle shape used, any appropriately large molecule will have multiple scattering events on its surface that are sufficient to result in an effectively diffuse collision (Wyttenbach, Bleiholder, & Bowers, 2013). Molecular Dynamics calculations in the presence of an electric field have been tested to calculate electrical mobilities in order to try and incorporate ro-vibrational degrees of freedom of gas and particles into the calculations (Lai, Dodds, & Li, 2018; Tamadate et al., 2019). While the results from these simulations are not as accurate as those of the DFT calculations, once the modeling parameters are optimized, they might become the new computational tool to study both the free molecular and transition regimes.

4. Conclusions

A consolidation effort to provide a coherent review of the various size-mobility relationships over the entire Knudsen range has been attempted. Despite the clear success of the different relations for spherical and non-spherical particles, and in particular of the Stokes-Millikan relationship, there is still a wide margin for improvements in accuracy and efficiency of the calculations, as well as in the conditions of applicability of the results. This is exceptionally true within the transition regime, for which no definitive computationally viable theory rooted only in fundamental principles is known and where experimentally derived parameters are still necessary to arrive at accurate mobility predictions. Given the success of numerical calculators within the free molecular regime and of DSMC calculators for much of the Knudsen range, it seems logical

that new calculators will soon become available with very accurate predictions within the transition regime. As more computational power becomes available, it is also logical to expect complex electrical mobility studies using Molecular Dynamics simulations that take into account the rotational and vibrational degrees of freedom of both charged particles and gas molecules. These studies will very likely shed some light into the specular vs. diffuse unresolved dilemma.

Overall, the study of electrical mobility and other transport properties in the field of aerosol science has reached a healthy maturity. With the emergence of increasingly accurate instrumentation and the rising need to better understand nucleation, coagulation and surface growth, as well as transport, filtration and toxicity of aerosol particles, aerosol science should make an effort to push the boundaries of the fundamental understanding of gas phase transport phenomena in the free molecular to transition region, a feat that, while not easy, is within the reach of the community.

5. Acknowledgements

Carlos Larriba-Andaluz would like to acknowledge support from the NSF Division of Chemistry under grant No. 1904879 (Prof. Kelsey Cook, Program Manager) and Kanomax Holdings Inc. for their support. Francesco Carbone would like to acknowledge support from the NSF CBET grant No. 2013382 (Prof. Harsha K. Chelliah, Program Manager).

6. About this Review

This article is an editor-invited review article. Editor-Invited review articles began in 2020 to commemorate the 50th anniversary of the Journal of Aerosol Science.

7. Biographies

Francesco Carbone is an Assistant Professor at the University of Connecticut. He earned his Ph.D. in Chemical Engineering and M.Sc. in Mechanical Engineering from the University of Naples Federico II (Italy) and got postgraduate training in Mechanical, Materials and Aerospace Engineering at Yale University and the University of Southern California. He is specialized in interrogating the detailed structure of reacting flows with a broad variety of experimental techniques and the assistance of modeling tools, and his studies contribute to the understanding of nanoparticle formation in flames.

Carlos Larriba-Andaluz got his bachelor's degree in Aerospace at the Universidad Politecnica de Madrid. He moved to the States after an abridged stay at Iberia Airlines. He got his Ph.D. in Mechanical Engineering from Yale University in 2010 followed by a postdoctoral Associate and Ramon Areces Fellow at the University of Minnesota in the department of Mechanical Engineering. In 2015 he started a tenure-track position at the Purdue University School of Engineering and Technology in Inidianapolis. His main area of research is steered towards Ion Mobility Spectrometry (IMS) coupled with Mass Spectrometry (MS).

References

Agarwal, P., & Girshick, S. L. (2012). Sectional modeling of nanoparticle size and charge distributions in dusty plasmas. *Plasma Sources Science and Technology, 21*(5), 055023.

Alam, M., & Flagan, R. (1986). Controlled nucleation aerosol reactors: production of bulk silicon. *Aerosol science and technology, 5*(2), 237-248.

Allen, M., & Raabe, O. (1982). Re-evaluation of Millikan's oil drop data for the motion of small particles in air. *Journal of Aerosol Science, 13*(6), 537-547.

Allen, M. D., & Raabe, O. G. (1985). Slip correction measurements of spherical solid aerosol particles in an improved Millikan apparatus. *Aerosol Science and Technology, 4*(3), 269-286.

Annis, B. (1971). Stress induced diffusion in monatomic gases and gas suspensions. *The Physics of Fluids, 14*(2), 269-277.

Annis, B., Malinauskas, A., & Mason, E. (1972). Theory of drag on neutral or charged spherical aerosol particles. *Journal of Aerosol Science, 3*(1), 55-64.

Annis, B., Malinauskas, A., & Yun, K. (1970). Composition Dependence of the Thermal-Diffusion Factor of a Dusty Gas. *The Journal of Chemical Physics, 52*(4), 1992-1996.

Basset, A. B. (1888). *A treatise on hydrodynamics: with numerous examples* (Vol. 2): Deighton, Bell and Company.

Bird, G. A. (1976). Molecular gas dynamics. *NASA STI/Recon Technical Report A, 76*.

Bleiholder, C., Wyttenbach, T., & Bowers, M. T. (2011). A novel projection approximation algorithm for the fast and accurate computation of molecular collision cross sections (I). Method. *International Journal of Mass Spectrometry, 308*(1), 1-10.

Bowden, F. P., & Harbour, P. (1966). The aerodynamic resistance to a sphere rotating at high Mach numbers in the rarefied transition regime. *Proceedings of the Royal Society of London. Series A. Mathematical and Physical Sciences, 293*(1433), 156-168.

Buckley, R., & Loyalka, S. (1989). Cunningham correction factor and accommodation coefficient: interpretation of Millikan's data. *Journal of aerosol science, 20*(3), 347-349.

Burgers, J. (1938). Second report on viscosity and plasticity. *Nordemann, New York*, 113.

Campuzano, I., Bush, M. F., Robinson, C. V., Beaumont, C., Richardson, K., Kim, H., & Kim, H. I. (2012). Structural characterization of drug-like compounds by ion mobility mass spectrometry: comparison of theoretical and experimentally derived nitrogen collision cross sections. *Analytical chemistry, 84*(2), 1026-1033.

Canzani, D., Laszlo, K. J., & Bush, M. F. (2018). Ion mobility of proteins in nitrogen gas: effects of charge state, charge distribution, and structure. *The Journal of Physical Chemistry A, 122*(25), 5625-5634.

Carbone, F., Canagaratna, M. R., Lambe, A. T., Jayne, J. T., Worsnop, D. R., & Gomez, A. (2019). Exploratory analysis of a sooting premixed flame via on-line high resolution (APi–TOF) mass spectrometry. *Proceedings of the Combustion Institute, 37*(1), 919-926.

Carrasco, B., & Garcıa de la Torre, J. (1999). Improved hydrodynamic interaction in macromolecular bead models. *The Journal of chemical physics, 111*(10), 4817-4826.

Cercignani, C., & Pagani, C. D. (1968). Flow of a rarefied gas past an axisymmetric body. I. General remarks. *The Physics of Fluids, 11*(7), 1395-1399.

Cercignani, C., Pagani, C. D., & Bassanini, P. (1968). Flow of a rarefied gas past an axisymmetric body. II. Case of a sphere. *The Physics of Fluids, 11*(7), 1399-1403.

Chahine, M. T. (1961). *Free molecule flow over non-convex surfaces.* Paper presented at the XIth International Astronautical Congress Stockholm 1960/XI. Internationaler Astronautischer Kongress/XIe Congrès International D'Astronautique.

Chan, P., & Dahneke, B. (1981). Free-molecule drag on straight chains of uniform spheres. *Journal of applied physics, 52*(5), 3106-3110.

Chang, C. W., Uhlenbeck, G., & de Boer, J. (1964). The Heat Conductivity and Viscosity of Poly-Atomic Gases: Studies in Statistical Mechanics: North-Holland Publishing Co., Amsterdam.

Chapman, S., & Cowling, T. G. (1970). *The mathematical theory of non-uniform gases: an account of the kinetic theory of viscosity, thermal conduction and diffusion in gases*: Cambridge university press.

Chen, Z. Y., Deutch, J., & Meakin, P. (1984). Translational friction coefficient of diffusion limited aggregates. *The Journal of chemical physics, 80*(6), 2982-2983.

Chen, Z. Y., Weakliem, P. C., & Meakin, P. (1988). Hydrodynamic radii of diffusion-limited aggregates and bond-percolation clusters. *The Journal of chemical physics, 89*(9), 5887-5889.

CHENG, Y.-S. (1991). Drag forces on nonspherical aerosol particles. *Chemical Engineering Communications, 108*(1), 201-223.

Coots, J., Gandhi, V., Onakoya, T., Chen, X., & Andaluz, C. L. (2020). A parallelized tool to calculate the electrical mobility of charged aerosol nanoparticles and ions in the gas phase. *Journal of Aerosol Science*, 105570.

Corson, J., Mulholland, G. W., & Zachariah, M. R. (2017). Friction factor for aerosol fractal aggregates over the entire Knudsen range. *Physical Review E, 95*(1), 013103.

Corson, J., Mulholland, G. W., & Zachariah, M. R. (2018). The effect of electric-field-induced alignment on the electrical mobility of fractal aggregates. *Aerosol Science and Technology, 52*(5), 524-535.

Cunningham, E. (1910). On the velocity of steady fall of spherical particles through fluid medium. *Proceedings of the Royal Society of London. Series A, Containing Papers of a Mathematical and Physical Character, 83*(563), 357-365.

Dahneke, B. (1983). Theory of dispersed multiphase flow: Academic Press, New York.

Dahneke, B. E. (1973a). Slip correction factors for nonspherical bodies—I Introduction and continuum flow. *Journal of Aerosol Science, 4*(2), 139-145.

Dahneke, B. E. (1973b). Slip correction factors for nonspherical bodies—II free molecule flow. *Journal of Aerosol Science, 4*(2), 147-161.

Dahneke, B. E. (1973c). Slip correction factors for nonspherical bodies—III the form of the general law. *Journal of Aerosol Science, 4*(2), 163-170.

Davies, C. (1945). Definitive equations for the fluid resistance of spheres. *Proceedings of the Physical Society, 57*(4), 259.

Davis, S. G., Joshi, A. V., Wang, H., & Egolfopoulos, F. (2005). An optimized kinetic model of H2/CO combustion. *Proceedings of the combustion Institute, 30*(1), 1283-1292.

de la Mora, J. F., De Juan, L., Liedtke, K., & Schmidt-Ott, A. (2003). Mass and size determination of nanometer particles by means of mobility analysis and focused impaction. *Journal of aerosol science, 34*(1), 79-98.

DeCarlo, P. F., Slowik, J. G., Worsnop, D. R., Davidovits, P., & Jimenez, J. L. (2004). Particle morphology and density characterization by combined mobility and aerodynamic diameter measurements. Part 1: Theory. *Aerosol Science and Technology, 38*(12), 1185-1205.

Derieux, J. B. (1918). The Use of Mercury Droplets in Millikan's Experiment. *Physical Review, 11*(3), 203.

Eglin, J. M. (1923). The coefficients of viscosity and slip of carbon dioxide by the oil drop method and the law of motion of an oil drop in carbon dioxide, oxygen, and helium, at low pressures. *Physical Review, 22*(2), 161.

Ehn, M., Junninen, H., Schobesberger, S., Manninen, H. E., Franchin, A., Sipilä, M., . . . Mirme, A. (2011). An instrumental comparison of mobility and mass measurements of atmospheric small ions. *Aerosol Science and Technology, 45*(4), 522-532.

Einstein, A. (1905). On the motion of small particles suspended in liquids at rest required by the molecular-kinetic theory of heat. *Annalen der physik, 17*(549-560), 208.

Epstein, P. S. (1924). On the resistance experienced by spheres in their motion through gases. *Physical Review, 23*(6), 710.

Ewing, S. A., Donor, M. T., Wilson, J. W., & Prell, J. S. (2017). Collidoscope: an improved tool for computing collisional cross-sections with the trajectory method. *Journal of The American Society for Mass Spectrometry, 28*(4), 587-596.

Fang, J., Wang, Y., Attoui, M., Chadha, T. S., Ray, J. R., Wang, W.-N., . . . Biswas, P. (2014). Measurement of sub-2 nm clusters of pristine and composite metal oxides during nanomaterial synthesis in flame aerosol reactors. *Analytical chemistry, 86*(15), 7523-7529.

Fernández-García, J., & de la Mora, J. F. (2013). Measuring the effect of ion-induced drift-gas polarization on the electrical mobilities of multiply-charged ionic liquid nanodrops in air. *Journal of the American Society for Mass Spectrometry, 24*(12), 1872-1889.

Fernández-García, J., & de la Mora, J. F. (2014). Electrical mobilities of multiply charged ionic-liquid nanodrops in air and carbon dioxide over a wide temperature range: Influence of ion-induced dipole interactions. *Physical Chemistry Chemical Physics, 16*(38), 20500-20513.

Fernández de la Mora, J. (2002). Free-molecule mobility of polyhedra and other convex hard-bodies. *Journal of aerosol science, 33*(3), 477-489.

Filippov, A. (2000). Drag and torque on clusters of N arbitrary spheres at low Reynolds number. *Journal of colloid and interface science, 229*(1), 184-195.

Friedlander, S. K. (2000). *Smoke, dust, and haze* (Vol. 198): Oxford University Press New York.

Fuchs, N. (1963). On the stationary charge distribution on aerosol particles in a bipolar ionic atmosphere. *Geofisica pura e applicata, 56*(1), 185-193.

Fuchs, N., Stechkina, I., & Starosselskii, V. (1962). On the determination of particle size distribution in polydisperse aerosols by the diffusion method. *British Journal of Applied Physics, 13*(6), 280.

Fuchs, N. A., Daisley, R., Fuchs, M., Davies, C., & Straumanis, M. (1965). The mechanics of aerosols. *Physics Today, 18*, 73.

Fuks, N. A., & Sutugin, A. G. (1970). Highly dispersed aerosols.

Gabelica, V., & Marklund, E. (2018). Fundamentals of ion mobility spectrometry. *Current opinion in chemical biology, 42*, 51-59.

Gamero-Castano, M., & de la Mora, J. F. (2002). Ion-induced nucleation: Measurement of the effect of embryo's size and charge state on the critical supersaturation. *The Journal of chemical physics, 117*(7), 3345-3353.

Garcia-Ybarra, P., & Rosner, D. E. (1989). Thermophoretic properties of nonspherical particles and large molecules. *AIChE Journal, 35*(1), 139-147.

Girshick, S. L., Chiu, C.-P., & McMurry, P. H. (1990). Time-dependent aerosol models and homogeneous nucleation rates. *Aerosol Science and Technology, 13*(4), 465-477.

Girshick, S. L., & Chiu, C. P. (1990). Kinetic nucleation theory: A new expression for the rate of homogeneous nucleation from an ideal supersaturated vapor. *The journal of chemical physics, 93*(2), 1273-1277.

Goldberg, R. (1954). *The Slow Flow of a Rarified Gas Past a Spherical Obstacle.* New York University, Graduate School of Arts and Science.

Goldstein, R. F. (1985). Macromolecular diffusion constants: a calculational strategy. *The Journal of chemical physics, 83*(5), 2390-2397.

Gopalakrishnan, R., & Hogan Jr, C. J. (2011). Determination of the transition regime collision kernel from mean first passage times. *Aerosol Science and Technology, 45*(12), 1499-1509.

Gopalakrishnan, R., & Hogan Jr, C. J. (2012). Coulomb-influenced collisions in aerosols and dusty plasmas. *Physical Review E, 85*(2), 026410.

Gopalakrishnan, R., Thajudeen, T., & Hogan Jr, C. J. (2011). Collision limited reaction rates for arbitrarily shaped particles across the entire diffusive Knudsen number range. *The Journal of chemical physics, 135*(5), 054302.

Gotts, N. G., von Helden, G., & Bowers, M. T. (1995). Carbon cluster anions: structure and growth from C5− to C62−. *International journal of mass spectrometry and ion processes, 149*, 217-229.

Happel, J., & Brenner, H. (2012). *Low Reynolds number hydrodynamics: with special applications to particulate media* (Vol. 1): Springer Science & Business Media.

Henderson, C. B. (1976). Drag coefficients of spheres in continuum and rarefied flows. *AIAA journal, 14*(6), 707-708.

Hinds, W. C. (1999). *Aerosol technology: properties, behavior, and measurement of airborne particles*: John Wiley & Sons.

Hirschfelder, J. O., Curtiss, C. F., Bird, R. B., & Mayer, M. G. (1964). *Molecular theory of gases and liquids* (Vol. 165): Wiley New York.

Hirsikko, A. E., Nieminen, T. J., Gagne, S., Lehtipalo, K., Manninen, H. E., Ehn, M. K., . . . McMurry, P. (2010). Atmospheric ions and nucleation: a review of observations. *Atmospheric Chemistry and Physics Discussions*.

Hohenberg, P., & Kohn, W. (1964). Inhomogeneous electron gas. *Physical review, 136*(3B), B864.

Hoppel, W., Frick, G., & Larson, R. (1986). Effect of nonprecipitating clouds on the aerosol size distribution in the marine boundary layer. *Geophysical Research Letters, 13*(2), 125-128.

Hubbard, J. B., & Douglas, J. F. (1993). Hydrodynamic friction of arbitrarily shaped Brownian particles. *Physical Review E, 47*(5), R2983.

Ieritano, C., Crouse, J., Campbell, J. L., & Hopkins, W. S. (2019). A parallelized molecular collision cross section package with optimized accuracy and efficiency. *Analyst, 144*(5), 1660-1670.

Iida, K., Stolzenburg, M., McMurry, P., Dunn, M. J., Smith, J. N., Eisele, F., & Keady, P. (2006). Contribution of ion-induced nucleation to new particle formation: Methodology and its application to atmospheric observations in Boulder, Colorado. *Journal of Geophysical Research: Atmospheres, 111*(D23).

Ishida, Y. (1923). Determination of viscosities and of the Stokes-Millikan law constant by the oil-drop method. *Physical Review, 21*(5), 550.

Ivanov, S., & Yanshin, A. (1980). Forces and moments acting on bodies rotating about a symmetry axis in a free molecular flow. *Fluid Dynamics, 15*(3), 449-453.

Jung, H., Han, K., Mulholland, G. W., Pui, D. Y., & Kim, J. H. (2013). Effect of the surface energy of particle materials on the accommodation of gas molecules to the particle surfaces. *Journal of aerosol science, 65*, 42-48.

Kihara, T. (1953). The mathematical theory of electrical discharges in gases. B. Velocity-distribution of positive ions in a static field. *Reviews of Modern Physics, 25*(4), 844.

Kilpatrick, W. (1971). *An experimental mass-mobility relation for ions in air at atmospheric pressure.* Paper presented at the Proc. Annu. Conf. Mass Spectrosc. 19th.

Kim, H., Kim, H. I., Johnson, P. V., Beegle, L. W., Beauchamp, J., Goddard, W. A., & Kanik, I. (2008). Experimental and theoretical investigation into the correlation between mass and ion mobility for choline and other ammonium cations in N2. *Analytical chemistry, 80*(6), 1928-1936.

Kirkwood, J. G., & Riseman, J. (1948). The intrinsic viscosities and diffusion constants of flexible macromolecules in solution. *The Journal of Chemical Physics, 16*(6), 565-573.

Knudsen, M. (1950). The Kinetic Theory of Gases, Methuen and Co. and John Wiley and Sons. *Inc., New York*.

Knudsen, M., & Weber, S. (1911). Luftwiderstand gegen die langsame Bewegung kleiner Kugeln. *Annalen der Physik, 341*(15), 981-994.

Knutson, E., & Whitby, K. (1975). Aerosol classification by electric mobility: apparatus, theory, and applications. *Journal of Aerosol Science, 6*(6), 443-451.

Kruger, C. H., & Vincenti, W. (1965). Introduction to physical gas dynamics. *John Wlley & Sons*.

Ku, B. K., & de la Mora, J. F. (2009). Relation between electrical mobility, mass, and size for nanodrops 1–6.5 nm in diameter in air. *Aerosol Science and Technology, 43*(3), 241-249.

Kulmala, M., Kontkanen, J., Junninen, H., Lehtipalo, K., Manninen, H. E., Nieminen, T., . . . Rantala, P. (2013). Direct observations of atmospheric aerosol nucleation. *Science, 339*(6122), 943-946.

Kusaka, I., Wang, Z. G., & Seinfeld, J. (1995). Ion-induced nucleation: A density functional approach. *The Journal of chemical physics, 102*(2), 913-924.

Laakso, L., Mäkelä, J. M., Pirjola, L., & Kulmala, M. (2002). Model studies on ion-induced nucleation in the atmosphere. *Journal of Geophysical Research: Atmospheres, 107*(D20), AAC 5-1-AAC 5-19.

Lai, R., Dodds, E. D., & Li, H. (2018). Molecular dynamics simulation of ion mobility in gases. *The Journal of chemical physics, 148*(6), 064109.

Landau, L., & Lifshitz, E. (1975). Fluid Mechanics 1st ed (Course of Theoretical Physics vol 6): Pergamon Press.

Langevin, M. (1905). *Une formule fondamentale de théorie cinétique.* Paper presented at the Annales de chimie et de physique, Series.

Larriba-Andaluz, C., Fernandez-Garcia, J., Ewing, M. A., Hogan, C. J., & Clemmer, D. E. (2015). Gas molecule scattering & ion mobility measurements for organic macro-ions in He versus N-2 environments. *Physical Chemistry Chemical Physics, 17*(22), 15019-15029.

Larriba-Andaluz, C., & Hogan, C. (2013). Novel interfaced approach to mobility calculations with diffuse scattering and Maxwell rotational distributions for diatomic gases in the free molecular regime. *Abstracts of Papers of the American Chemical Society, 246*.

Larriba-Andaluz, C., Nahin, M., & Shrivastav, V. (2017). A contribution to the amaranthine quarrel between true and average electrical mobility in the free molecular regime. *Aerosol Science and Technology, 51*(7), 887-895.

Larriba, C., & Fernandez de la Mora, J. (2012). The gas phase structure of coulombically stretched polyethylene glycol ions. *The Journal of Physical Chemistry B, 116*(1), 593-598.

Larriba, C., & Hogan, C. J. (2013a). Free molecular collision cross section calculation methods for nanoparticles and complex ions with energy accommodation. *Journal of Computational Physics, 251*, 344-363.

Larriba, C., & Hogan, C. J. (2013b). Ion Mobilities in Diatomic Gases: Measurement versus Prediction with Non-Specular Scattering Models. *Journal of Physical Chemistry A, 117*(19), 3887-3901.

Larriba, C., Hogan Jr, C. J., Attoui, M., Borrajo, R., Garcia, J. F., & De La Mora, J. F. (2011). The mobility–volume relationship below 3.0 nm examined by tandem mobility–mass measurement. *Aerosol Science and Technology, 45*(4), 453-467.

Lassalle, L. J. (1921). On the motion of a sphere of oil through carbon dioxide and a determination of the coefficient of viscosity of that gas by the oil drop method. *Physical Review, 17*(3), 354.

Law, W., & Loyalka, S. (1986). Motion of a sphere in a rarefied gas. II. Role of temperature variation in the Knudsen layer. *The Physics of fluids, 29*(11), 3886-3888.

Lea, K., & Loyalka, S. (1982). Motion of a sphere in a rarefied gas. *The Physics of Fluids, 25*(9), 1550-1557.

Leaptrot, K. L., May, J. C., Dodds, J. N., & McLean, J. A. (2019). Ion mobility conformational lipid atlas for high confidence lipidomics. *Nature communications, 10*(1), 1-9.

Lee, J. Y. (1914). Determination of the Value of" e," by Millikan'S Method, Using Solid Spheres. *Physical Review, 4*(5), 420.

Lenard, P., Weick, W., & Mayer, H. F. (1920). Über Elektrizitätsleitung durch freie Elektronen und Träger. III: Wanderungsgeschwindigkeit kraftgetriebener Partikel in reibenden Medien, mit Beiträgen von W. Weick und Hans Ferd. Mayer. *Annalen der Physik, 366*(8), 665-741.

Li, C., Singh, N., Andrews, A., Olson, B. A., Schwartzentruber, T. E., & Hogan Jr, C. J. (2019). Mass, momentum, and energy transfer in supersonic aerosol deposition processes. *International Journal of Heat and Mass Transfer, 129*, 1161-1171.

Li, M., Mulholland, G. W., & Zachariah, M. R. (2014). Understanding the mobility of nonspherical particles in the free molecular regime. *Physical Review E, 89*(2), 022112.

Li, Z.-H., Peng, A.-P., Zhang, H.-X., & Yang, J.-Y. (2015). Rarefied gas flow simulations using high-order gas-kinetic unified algorithms for Boltzmann model equations. *Progress in Aerospace Sciences, 74*, 81-113.

Li, Z., & Wang, H. (2003a). Drag force, diffusion coefficient, and electric mobility of small particles. I. Theory applicable to the free-molecule regime. *Physical Review E, 68*(6), 061206.

Li, Z., & Wang, H. (2003b). Drag force, diffusion coefficient, and electric mobility of small particles. II. Application. *Physical Review E, 68*(6), 061207.

Li, Z., & Wang, H. (2005). Gas-nanoparticle scattering: A molecular view of momentum accommodation function. *Physical review letters, 95*(1), 014502.

Liu, C., & Sugimura, T. (1969). Rarefied gas flow over a sphere at low Mach numbers.

Liu, V. C., Pang, S. C., & Jew, H. (1965). Sphere Drag in Flows of Almost-Free Molecules. *The Physics of Fluids*, *8*(5), 788-796.

Loth, E. (2008). Compressibility and rarefaction effects on drag of a spherical particle. *AIAA journal*, *46*(9), 2219-2228.

Mackowski, D. W. (2006). Monte Carlo simulation of hydrodynamic drag and thermophoresis of fractal aggregates of spheres in the free-molecule flow regime. *Journal of aerosol science*, *37*(3), 242-259.

Mason, E., & Hahn, H.-s. (1972). Ion drift velocities in gaseous mixtures at arbitrary field strengths. *Physical Review A*, *5*(1), 438.

Mason, E., Malinauskas, A., & Evans Iii, R. (1967). Flow and diffusion of gases in porous media. *The Journal of Chemical Physics*, *46*(8), 3199-3216.

Mason, E. A., & Chapman, S. (1962). Motion of small suspended particles in nonuniform gases. *The Journal of Chemical Physics*, *36*(3), 627-632.

Mason, E. A., & McDaniel, E. W. (1988). *Transport properties of ions in gases*. New York: John Wiley & Sons.

Mason, E. A., & Schamp Jr, H. W. (1958). Mobility of gaseous lons in weak electric fields. *Annals of physics*, *4*(3), 233-270.

Mattauch, J. (1925). Eine experimentelle Ermittlung des Widerstandsgesetzes kleiner Kugeln in Gasen. *Zeitschrift für Physik*, *32*(1), 439-472.

Matz, L. M., Hill, H. H., Beegle, L. W., & Kanik, I. (2002). Investigation of drift gas selectivity in high resolution ion mobility spectrometry with mass spectrometry detection. *Journal of the American Society for Mass Spectrometry*, *13*(4), 300-307.

Mazur, P., & van Saarloos, W. (1982). Many-sphere hydrodynamic interactions and mobilities in a suspension. *Physica A: Statistical Mechanics and its Applications*, *115*(1-2), 21-57.

McCoy, B., & Cha, C. (1974). Transport phenomena in the rarefied gas transition regime. *Chemical Engineering Science*, *29*(2), 381-388.

McDaniel, E. W., & Mason, E. A. (1973). Mobility and diffusion of ions in gases.

McMurry, P. (1983). New particle formation in the presence of an aerosol: Rates, time scales, and sub-0.01 μm size distributions. *Journal of colloid and interface science*, *95*(1), 72-80.

Meakin, P., Chen, Z. Y., & Deutch, J. (1985). The translational friction coefficient and time dependent cluster size distribution of three dimensional cluster–cluster aggregationa), b). *The Journal of chemical physics*, *82*(8), 3786-3789.

Melas, A. D., Isella, L., Konstandopoulos, A. G., & Drossinos, Y. (2014). Friction coefficient and mobility radius of fractal-like aggregates in the transition regime. *Aerosol Science and Technology*, *48*(12), 1320-1331.

Melas, A. D., Isella, L., Konstandopoulos, A. G., & Drossinos, Y. (2015). A methodology to calculate the friction coefficient in the transition regime: Application to straight chains. *Journal of Aerosol Science*, *82*, 40-50.

Mesleh, M. F., Hunter, J. M., Shvartsburg, A. A., Schatz, G. C., & Jarrold, M. F. (1996). Structural information from ion mobility measurements: Effects of the long-range potential. *Journal of Physical Chemistry*, *100*(40), 16082-16086.

Metzig, G. (1984). The motion of small particles in air—a new approach based on thereflection mode'of molecules. *JAerS*, *15*(3), 256-258.

Millikan, R. (1920). The resistance of a gas to the motion of a sphere when the mean free path is large in comparison with the diameter of the sphere. *Phys. Rev*, *15*, 544-545.

Millikan, R. A. (1911). The Isolation of an Ion, a Precision Measurement of its Charge, and the Correction of Stokes's Law. *Physical Review (Series I)*, *32*(4), 349.

Millikan, R. A. (1923a). Coefficients of slip in gases and the law of reflection of molecules from the surfaces of solids and liquids. *Physical review*, *21*(3), 217.

Millikan, R. A. (1923b). The general law of fall of a small spherical body through a gas, and its bearing upon the nature of molecular reflection from surfaces. *Physical Review*, *22*(1), 1.

Mönch, G. C. (1933). Zum Widerstandsgesetz kleiner Kugeln in Luft. *Zeitschrift für Physik*, *34*, 77.

Monchick, L., Pereira, A., & Mason, E. (1965). Heat conductivity of polyatomic and polar gases and gas mixtures. *The Journal of Chemical Physics, 42*(9), 3241-3256.

Monchick, L., Yun, K., & Mason, E. (1963). Formal kinetic theory of transport phenomena in polyatomic gas mixtures. *The Journal of Chemical Physics, 39*(3), 654-669.

Ouyang, H., Larriba-Andaluz, C., Oberreit, D. R., & Hogan, C. J. (2013). The Collision Cross Sections of Iodide Salt Cluster Ions in Air via Differential Mobility Analysis-Mass Spectrometry. *Journal of the American Society for Mass Spectrometry, 24*(12), 1833-1847.

Ouyang, H., Larriba-Andaluz, C., Oberreit, D. R., & Hogan Jr, C. J. (2013). The collision cross sections of iodide salt cluster ions in air via differential mobility analysis-mass spectrometry. *Journal of the American Society for Mass Spectrometry, 24*(12), 1833-1847.

Pao, Y. p., & Willis, D. R. (1969). Asymptotic Theory of Nearly Free-Molecular Flows. *The Physics of Fluids, 12*(2), 435-446.

Phillips, W. F. (1975). Drag on a small sphere moving through a gas. *The Physics of Fluids, 18*(9), 1089-1093.

Pratsinis, S. E. (1988). Simultaneous nucleation, condensation, and coagulation in aerosol reactors. *Journal of Colloid and Interface Science, 124*(2), 416-427.

Rader, D. J. (1990). Momentum slip correction factor for small particles in nine common gases. *Journal of aerosol science, 21*(2), 161-168.

Reuland, P., Felderhof, B., & Jones, R. (1978). Hydrodynamic interaction of two spherically symmetric polymers. *Physica A: Statistical Mechanics and its Applications, 93*(3-4), 465-475.

Rogak, S. N., & Flagan, R. C. (1992). Coagulation of aerosol agglomerates in the transition regime. *Journal of Colloid and Interface Science, 151*(1), 203-224.

Rose, M. H. (1964). Drag on an Object in Nearly-Free Molecular Flow. *The Physics of Fluids, 7*(8), 1262-1269.

Rotne, J., & Prager, S. (1969). Variational treatment of hydrodynamic interaction in polymers. *The Journal of Chemical Physics, 50*(11), 4831-4837.

Schmitt, K. H. (1959). Untersuchungen an schwebstoffteilchen im temperaturfeld. *Zeitschrift für Naturforschung A, 14*(10), 870-881.

Shrivastav, V., Nahin, M., Hogan, C. J., & Larriba-Andaluz, C. (2017a). Benchmark comparison for a multi-processing ion mobility calculator in the free molecular regime. *Journal of the American Society for Mass Spectrometry, 28*(8), 1540-1551.

Shrivastav, V., Nahin, M., Hogan, C. J., & Larriba-Andaluz, C. (2017b). Benchmark Comparison for a Multi-Processing Ion Mobility Calculator in the Free Molecular Regime. *Journal of The American Society for Mass Spectrometry*, 1-12.

Shvartsburg, A. A., & Jarrold, M. F. (1996). An exact hard-spheres scattering model for the mobilities of polyatomic ions. *Chemical physics letters, 261*(1-2), 86-91.

Silvey, O. (1916). The fall of mercury droplets in a viscous medium. *Physical Review, 7*(1), 106.

Smoluchowski, M. (1906). The kinetic theory of Brownian molecular motion and suspensions. *Ann. Phys, 21*, 756-780.

Sorensen, C. (2011). The mobility of fractal aggregates: a review. *Aerosol Science and Technology, 45*(7), 765-779.

Stacy, L. J. (1923). A determination by the constant deflection method of the value of the coefficient of slip for rough and for smooth surfaces in air. *Physical Review, 21*(3), 239.

Stokes, G. G. (1851). *On the effect of the internal friction of fluids on the motion of pendulums* (Vol. 9): Pitt Press Cambridge.

Sugimura, T. (1968). Rarefied Gas Flow over a Sphere.

Takata, S., Sone, Y., & Aoki, K. (1993). Numerical analysis of a uniform flow of a rarefied gas past a sphere on the basis of the Boltzmann equation for hard-sphere molecules. *Physics of Fluids A: Fluid Dynamics, 5*(3), 716-737.

Tamadate, T., Orii, T., Higashi, H., Otani, Y., Kumita, M., & Seto, T. (2019). Conformation-dependent dynamics of macromolecular ions in the gas phase under an electrostatic field: A molecular dynamics simulation. *Aerosol Science and Technology, 53*(3), 260-267.

Tammet, H. (1995). Size and mobility of nanometer particles, clusters and ions. *Journal of Aerosol Science, 26*(3), 459-475.

Van Dyke, K. S. (1923). The coefficients of viscosity and of slip of air and of carbon dioxide by the rotating cylinder method. *Physical Review, 21*(3), 250.

Veshchunov, M. (2010a). A new approach to the Brownian coagulation theory. *Journal of aerosol science, 41*(10), 895-910.

Veshchunov, M. (2010b). On the theory of Brownian coagulation. *Journal of Engineering Thermophysics, 19*(2), 62-74.

Viehland, L. A., & Mason, E. (1975). Gaseous lon mobility in electric fields of arbitrary strength. *Annals of Physics, 91*(2), 499-533.

Viehland, L. A., & Mason, E. (1978). Gaseous ion mobility and diffusion in electric fields of arbitrary strength. *Annals of Physics, 110*(2), 287-328.

Viehland, L. A., & Mason, E. A. (1995). Transport Properties of Gaseous-Ions over a Wide Energy-Range .4. *Atomic Data and Nuclear Data Tables, 60*(1), 37-95. doi: DOI 10.1006/adnd.1995.1004

Von Helden, G., Hsu, M. T., Kemper, P. R., & Bowers, M. T. (1991). Structures of carbon cluster ions from 3 to 60 atoms: Linears to rings to fullerenes. *The journal of chemical physics, 95*(5), 3835-3837.

Waldmann, L. (1959). Über die Kraft eines inhomogenen Gases auf kleine suspendierte Kugeln. *Zeitschrift für Naturforschung A, 14*(7), 589-599.

Wannier, G. H. (1953). Motion of gaseous ions in strong electric fields. *The Bell System Technical Journal, 32*(1), 170-254.

Wiedensohler, A. (1988). An approximation of the bipolar charge distribution for particles in the submicron size range. *Journal of aerosol science, 19*(3), 387-389.

Wu, T. Y., Derrick, J., Nahin, M., Chen, X., & Larriba-Andaluz, C. (2018). Optimization of long range potential interaction parameters in ion mobility spectrometry. *Journal of Chemical Physics, 148*(7). doi: Artn 074102 10.1063/1.5016170

Wyttenbach, T., Bleiholder, C., & Bowers, M. T. (2013). Factors contributing to the collision cross section of polyatomic ions in the kilodalton to gigadalton range: application to ion mobility measurements. *Analytical chemistry, 85*(4), 2191-2199.

Yamakawa, H. (1970). Transport properties of polymer chains in dilute solution: hydrodynamic interaction. *The Journal of Chemical Physics, 53*(1), 436-443.

Zanotto, L., Heerdt, G., Souza, P. C., Araujo, G., & Skaf, M. S. (2018). High performance collision cross section calculation—HPCCS. *Journal of computational chemistry, 39*(21), 1675-1681.

Zhang, C., Thajudeen, T., Larriba, C., Schwartzentruber, T. E., & Hogan Jr, C. J. (2012). Determination of the scalar friction factor for nonspherical particles and aggregates across the entire Knudsen number range by direct simulation Monte Carlo (DSMC). *Aerosol Science and Technology, 46*(10), 1065-1078.

Zurita-Gotor, M. (2006). Size-and structure-independence of the thermophoretic transport of an aerosol particle for specular boundary conditions in the free molecule regime. *Journal of aerosol science, 37*(3), 283-291.

Zurita-Gotor, M., & Rosner, D. (2002). Effective diameters for collisions of fractal-like aggregates: Recommendations for improved aerosol coagulation frequency predictions. *Journal of colloid and interface science, 255*(1), 10-26.

Zurita, G. M. (2004). Rational numerical simulations in sol reaction engineering.